ISSN 0869-5911, Petrology, 2010, Vol. 18, No. 5, pp. 489–513. © Pleiades Publishing, Ltd., 2010.
Original Russian Text © Yu.A. Martynov, A.I. Khanchuk, J.-I. Kimura, A.V. Rybin, A.Yu. Martynov, 2010, published in Petrologiya, 2010, Vol. 18, No. 5, pp. 512–535

Geochemistry and Petrogenesis of Volcanic Rocks in the Kuril Island Arc

Yu. A. Martynov [a], A. I. Khanchuk [a], J.-I. Kimura [b], A. V. Rybin [c], and A. Yu. Martynov [a]

[a] *Far East Geological Institute, Far East Division, Russian Academy of Sciences, pr. Stoletiya Vladivostoka 159, Vladivostok, 660022 Russia*
e-mail: martynov@fegi.ru

[b] *Institute for Research on Earth Evolution, Japan Agency for Marine—Earth Science and Technology, Yokusuka 237-0061, Japan*
e-mail: jkimura@jamstec.go.jp

[c] *Institute of Marine Geology and Geophysics, Far East Division, Russian Academy of Sciences, ul. Nauki 5, Yuzhno-Sakhalinsk, 6930022 Russia*
e-mail: rybin@imgg.ru

Received September 27, 2009; in final form, December 2, 2009

Abstract—Newly obtained precise analytical data on trace elements and radiogenic Sr, Nd, and Pb isotopes testify to anomalous geochemical characteristics of mafic and intermediate Quaternary lavas in Paramushir (in the north of the Kuril arc), Kunashir and Iturup (in the south) islands, which are the largest three islands of the Kuril island arc. The high K and LREE concentrations in the volcanic products in Paramushir Island resulted from the southward expansion of the mantle thermal anomaly of the Kamchatka Peninsula and the involvement of melts related to the melting of oceanic sediments in magma generation. The depleted characteristics of the mafic volcanics are explained by the relatively young tectono-magmatic events during the opening of the Kuril backarc basin. The Kuril island-arc system developed on a heterogeneous basement. The northern islands are a continuation of the volcanic structures of southern Kamchatka, which were formed above an isotopically depleted and hot lithospheric mantle domain of composition close to that of the Pacific MORB type. The southern islands were produced above an isotopically enriched and cold lithospheric domain of the Indian-Ocean MORB type, which was modified in relation to relatively young backarc tectono-magmatic processes. Although issues related to the genesis of the transverse geochemical zoning were beyond the originally formulated scope of our research, the homogeneous enough isotopic composition of the rear-arc lavas in the absence of any mineralogical and geochemical lines of evidence of crustal contamination suggest an independent magmatic source.

DOI: 10.1134/S0869591110050048

INTRODUCTION

Island-arc systems are key structural elements in plate tectonics, zones of active interaction of crustal and mantle material and the origin of new deep geochemical reservoirs. Although these structures attracted keen attention of many researchers, many aspects of their "action" remain uncertain so far. This fully pertains to magmatic rocks, whose genesis is much more complicated than that of, for example, basalts in mid-oceanic ridges (MORB) or oceanic islands (OIB). In additions to the suprasubduction mantle, arc-related magma generation is significantly contributed by subducted material produced by the dehydration or melting of the oceanic crust and sediments. A further uncertainty is introduced by "off-subduction" factors, such as variations in the geodynamic regime, the heterogeneity of the lithospheric mantle (Arculus, 1994; Pearce et al., 2005; and others), crustal contamination (see, for example, Kimura and Yoshida, 2006), and the activity of backarc tectono-magmatic processes (Pearce and Parkinson, 1993; and others) and faulting (Avdeiko et al., 2001).

One of the most important tools used to evaluate the contribution of various components to magma generation is studying the spatiotemporal variations in the composition of magmatic rocks. Regretfully, information of this type on the Kurils is still sparse (Bailey, 1996; Ishikawa and Tera, 1997). In this publications, issues related to the longitudinal and transverse lateral zoning of the Quaternary volcanics are considered based on trace-element and isotopic data recently obtained with the use of state-of-the-art analytical techniques.

The island arc system of northeastern Japan and the Kurils were formed in the Late Cenozoic on the eastern margin of the Eurasian continent, in association with backarc marine basins of the seas of Japan and Okhotsk. While subduction processes in northeastern Japan were examined exhaustively enough and involved studying magmatic occurrences related to the opening of the backarc basin (Goto et al., 1995; Kimura and Yoshida, 2006; Okamura et al., 1998, 2005; and others), the Kuril island arc was inspected much less thoroughly. The very first monograph summarizing geophysical, geological, petrographic, and petrochemical data was published by Gorshkov (1967), but now it is not of any interest except only as a source of detailed descriptions of the morphologies and inner structures of principally important volcanic centers. Comparing vertical geological sections of volcanic and volcanic–sedimentary rocks, Piskunov (1987) has distinguished regional volcanic complexes and evaluated the parameters of their origin. Fedorchenko et al. (1989) reviewed data on the distribution and composition of xenoliths in the Quaternary lavas.

Information on the trace-element and, particularly, isotopic composition of the Quaternary volcanics is sparse and pertains to a few volcanic centers (Bailey et al., 1989; Matynov et al., 2005). After the pioneering paper by Zhuravlev et al. (1985), newly obtained isotopic data were published only for certain volcanoes in Iturup Island (Bindeman and Bailey, 1999) and the adjacent territory of the Kuril Basin. Thereby data on the Pb isotopic composition are practically absent.

Problems of the magma genesis of Kuril lavas were explored most exhaustively and based on the most recent analytical material in (Ishikawa and Tera, 1997). Noting a linear correlation of $\delta^{11}B$ with $^{87}Sr/^{86}Sr$ and Nb/B, these researchers believed that the transverse geochemical zoning is related to the mixing of two isotopically homogeneous components: subduction fluid and a mantle-wedge material. With regard for the relatively high Nb/B ratios in the two samples of backarc volcanics from the central and southern links, we cannot rule out that juvenile mantle material could contribute to the generation of the magmas. An important role of a fluid phase in the origin of magmatic rocks in the frontal zone was emphasized in (Zhuravlev et al., 1985; Bogatikov and Tsvetkov, 1988; *Submarine Volcanism…*, 1992; Bindeman and Bailey, 1999). Some researchers (*Submarine Volcanism…*, 1992; Bindeman and Bailey, 1999) suggested that the composition of the magma source systematically changed toward the rear zone of the island arc.

The weak longitudinal geochemical zoning of the Kuril island arc, with the variation in the composition of the volcanics from the predominant high-K to moderate-K types (Popolitov and Volynets, 1982; Bailey et al., 1989; *Submarine Volcanism…*, 1992) were interpreted as resulting from the insignificant difference between the lithologies of the subduction sediments in the northern and southern segments (Bailey, 1996; Ishikawa and Terry, 1997). The authors of (*Submarine Volcanism…*, 1992) placed accent onto the localization of lavas with elevated potassic alkalinity at junction zones of variably oriented arc flanks in the northern (Paramushir Island) and central (Simushir island) parts of the arc.

GEOLOGICAL OVERVIEW

The Kuril island arc system consists of the Kuril–Kamchatka trench, Greater Kuril volcanic islands, and Kuril Basin (Fig. 1). At a constant convergence velocity of approximately 8.6 km/year, the age of the oceanic crust near the Kuril–Kamchatka trench varies from 90 to 118 Ma and becomes older southward. The old age of the oceanic slab is correlated with the maximum depth of earthquakes (up to 650 km). All segments of the island arc are classed with zones of moderate contraction (Bailey, 1996).

The Kuril–Kamchatka Trench is filled with oceanic sediments with variable admixtures of continental material (17–80 vol %), siliceous biogenic material (approximately 9 vol %), volcanic ash (a few volume percent), and minor amounts of carbonates. The percentage of continental material in the sediments increases southward (Ishikawa and Tera, 1997).

The Gerater Kuril island arc started to develop in the Early Miocene or Oligocene. It extends for more than 1150 km at a width from 100 to 200 km. The arc is traditionally subdivided into northern, central, and southern zones or sectors (Fig. 1). The surface of the downgoing Pacific plate is located beneath the volcanic front at a depth of 94.2 km (southern sector) to 92 km (northern sector) Syracuse and Abers, 2006). The crustal thickness varies insignificantly (from 28 to 33 km in the southern zone, from 25 to 30 km in the central zone, and from 32 to 36 km in the northern zone) (Zlobin, 1987). In addition to a significant thickness, the continental nature of the crust follows from the occurrence of xenoliths of metamorphic rocks (plagioclase–pyroxene granulites and crystalline schists) throughout the whole arc (*Submarine Volcanism…*, 1992). The volcanic front is dominated by olivine–pyroxene gabbroids (gabbro, gabbronorites, and gabbro-anorthosites) and contains subordinate amounts of allivalites, troctolites, eucrites, and granitoids (in Paramushir, Simushir, and Kunashir islands). The rear zone contains amphibole gabbro and hyperbasites. Gabbroid and metamorphic-rock nodules in the rear-arc lavas are enriched in Ti, alkalis, Rb, Ba, Sr, Ni, Cr, and Zn but depleted in Cr, V, Pb, and Sn (*Submarine Volcanism…*, 1992).

The volcanic and volcanic–sedimentary rocks composing the islands are subdivided into two structural floors. The lower floor consists of moderately deformed Late Cenozoic rocks (Early–Middle Miocene–Pliocene), and the upper one is made up of Quaternary Pleistocene–Holocene volcanics. Volcanic rocks of both structural floors vary in composition from basalt to rhyolite at the predominance of basalts and andesites (*Submarine Volcanism…*, 1992).

The Kuril Basin is though to have been formed in the Early–Middle Miocene (32–15 Ma). Its shape (an irregular triangle with pitching-outs near the boundary between the central and northern sectors, near the island of Shiashkotan; Fig. 1) suggests that the exten-

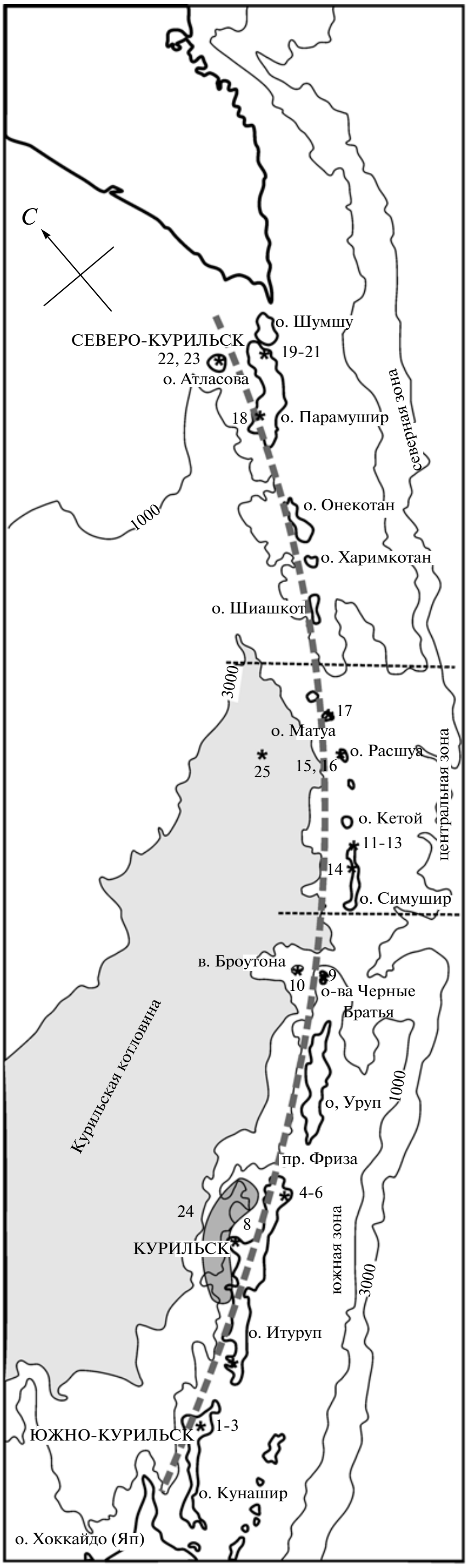

Fig. 1. Schematic map of the Kuril Islands and Kuril backarc basin.

Numerals denote volcanoes: (*1–3*) Tyatya, (*4–6*) Men'shoi Brat, (*7*) L'vinaya Past', (*8*) Bogdan Khmel'nitskii, (*9*) Brat Cherpoev, (*10*) Broutona, (*11–13*) Uratman, (*14*) Prevo, (*15, 16*) Rasshua, (*17*) Sarycheva, (*18*) Chikurachki, (*19, 20*) Ebeko, (*22, 23*) Alaid; (*24*) field of relatively small submarine volcanoes behind Iturup Island (Bindeman and Bailey, 1999), (*25*) Geofizikov submarine volcano (Baranov et al., 2002).

Black and thin dashed lines show the boundaries of the southern, central, and northern sectors, and the gray line demarks the boundary between frontal-arc and rear-arc Quaternary volcanic rocks. Note that most of the sampled volcanoes belong to the frontal zone.

Key: 1. N; 2. Severo-Kuril'sk; 3. Atlasova Isl.; 4. Shumshu Isl.; 5. Paramushir Isl.; 6. Onekotan Isl.; 7. northern zone; 8. Kharimkotan Isl.; 9. Shiashkotan Isl.; 10. Matua Isl.; 11. Rasshua Isl.; 12. Ketoi Isl.; 13. Simushir Isl.; 14. central zone; 15. Broutona Isl.; 16. Kuril Basin; 17. Chernye Brat'ya Isls.; 18. Urup Isl.; 19. Friza Isl.; 20. southern zone; 21. Kuril'sk; 22. Iturup Isl.; 23. Yuzhno-Kuril'sk; 24. Kunashir Isl.; 25. Hokkaido (Japan)

sion processes in the south and north of the backarc structure have different intensity. In spite of the transition from a compressional to extensional environment (Baranov et al., 2002), magmatic processes in the rear zone remain active until nowadays, as follows form the high heat flux (up to 105 mW/m^2) and the occurrence of Quaternary (0.84–1.07 Ma) submarine volcanic rocks (Baranov et al., 2002; Tararin et al., 2000).

ANALYTICAL TECHNIQUES

Approximately 200 representative samples of the Quaternary lavas were analyzed for major and trace elements. Concentrations of major elements were determined at the Laboratory of Analytical Chemistry at the Far East Geological Institute, Far East Division, Russian Academy of Sciences, using gravimetry (SiO_2) and inductively coupled plasma atomic emission spectrometry (TiO_2, Al_2O_3, $Fe_2O_3^*$, CaO, MgO, MnO, K_2O, Na_2O, and P_2O_5) on an ICAP 6500 Duo (Thermo Electron Corporation, United States) spectrometer. The internal standard was Cd (10 ppm Cd concentration) solution (analysts V.N. Kaminskaya, M.G. Blokhin, and G.I. Gorbach). Considering the predominantly mafic composition of the rocks and their relatively low concentrations of alkalis, the samples were dissolved by means of open acid decomposition in a mixture of HF, HNO_3, and $HClO_4$ ("superapure", Merc) in the proportion 2.5 : 1 : 0.5 (Smirnova et al., 2003). The calibration solutions were prepared from standard samples of the composition DVA, DVB, DVD, DVR, and SA-1 (Russia) by means of open decomposition.

Some trace elements (LI, Be, Sc, V, Co, Cr, Ni, Zn, Ga, Rb, Sr, Y, Zr, Nb, Mo, Cd, Cs, Ba, REE, Hf, Ta, W, Pb, Th, and U) were analyzed by ICP-MS on an Agilent 7500 (Agilent Technologies, United States) quadrupole mass spectrometer, with ^{115}In as the internal standard (the final concentration in the solution was 10 ppb). The analyzer was calibrated using certified multielement solutions CLMS-1, CLMS-2, CLMS-3, and CLMS-4 (United States); the standards were geological samples of basalts JB-2 and JB-3 and andesite JA-2 (Japan).

The trace-element composition of the samples was analyzed at the Irkutsk Analytical Center of Collective Usage on a VG Plasmaquad PQ2+ mass spectrometer, which was calibrated on internationally certified standards BHVO-1, AGV-1, and BIR-1 at the continuous internal laboratory control of the quality of the analyses against basanite sample U-94-5, which was analyzed by ICP-MS at the Royal Museum of Central Africa in Belgium. The chemical preparation of the samples was carried out with the application of doubly distilled deep water from Lake Baikal and with acid doubly purified by isothermal distillation; HF was purified in Teflon vessels, and H_2O, HNO_3, and HCl were purified in quartz vessels.

Analyses of replicate samples conducted at two different analytical centers showed a good consistency.

Forty samples were analyzed for Sr, Nd, and Pb radiogenic isotopes at the Shimane University in Matsue, Japan, on a multocollector ICP-MS (Thermo Elemental VG Plasma 54), with the use of ultrapure acid reactants. The techniques applied to concentrate Sr, Nd, and Pb was described in (Iizumi et al., 1994, 1995; Kimura et al., 2003).

GEOCHEMISTRY

Major Elements

The SiO_2 and MgO concentrations in Quaternary lavas from the Kuril island arc vary from 47 to 75 and from 1 to 10 wt %, respectively (table). The low TiO_2 (<1 wt %) and high Al_2O_3 (15–25 wt %) concentrations suggest a suprasubduction nature of all of our rock samples. A decrease in the MgO concentrations is associated with an increase in the concentrations of SiO_2, Na_2O, and K_2O and a decrease in the CaO concentration. The variations in the TiO_2 concentration are insignificant. At MgO < 7–4 wt %, the Al_2O_3 concentrations of our samples drastically increase to 20–22 wt % or gradually decrease to 15–16 wt % (Fig. 2).

Volcanic rocks from the frontal and rear zones are clearly different in a number of petrochemical features. The former are characterized by significant variations in silicity (from ~46 to ~70 wt % SiO_2) and MgO concentrations (Fig. 2). The MgO concentration in some samples from the frontal zone of the southern sector (Kunashir and Iturup islands) are as high as 9–14 wt %, and this makes it possible to regard these rocks as primary mantle partial melts. Lavas from the frontal zone usually plot within the field of the low-K series in the SiO_2–K_2O classification diagram (Fig. 3) and in the field of the calc–alkaline series in the SiO_2–FeO*/MgO diagram (Fig. 4).

The compositions of the volcanics display clearly discernible longitudinal variations, first of all, in the concentrations of K_2O and, to a lesser degree, MgO. Lavas from the southern islands are noted for low (for rocks in the frontal zones of island arc systems) K_2O concentrations, which are anomalously high in lavas from Paramushir Island. Lavas from Kunashir and Iturup islands are characterized by the occurrence of high-Mg varieties (MgO > 10 wt %). No variations are usually observed in the concentrations of other major oxides, including Na_2O and TiO_2.

The rear-arc rocks typically show limited compositional variations and are dominated by basalts and basaltic andesites (50–55 wt % SiO_2). The MgO concentrations range from 3 to 7 wt % (Fig. 2). More magnesian lavas (7–9 wt % MgO) were found in the rear zone of Iturup Island. In the northern sector (Atlasovo Island), the MgO variations are constrained to the range of 3–6 wt %, although occasional samples contain up to 8 wt % MgO. The K_2O concentrations in volcanics from the southern and central sectors correspond to those in the moderate-K series, and the variations in these concentrations in rocks from the northern sector are as in the high-K series. In the SiO_2–FeO*/MgO diagram (Fig. 4), the data points of the rear-arc volcanics lie mostly within the tholeiite field, and the overlap zone with the front-arc lavas is insignificant. Having similar MgO concentrations, the rear-arc lavas usually have higher K_2O, TiO_2, Na_2O, CaO, and Al_2O_3 contents and lower SiO_2 concentrations than those in the front-arc volcanics (Fig. 2).

The longitudinal zoning of the rear zone is pronounced not as clearly, perhaps, because our collection of rock samples is not as representative, although the K_2O concentrations are prone to increase northward at a simultaneous decrease in the MgO concentrations of the rocks.

Trace Elements

According to their trace-element characteristics, Quaternary volcanics from the Kuril island arc are typical suprasubduction rocks with relatively high concentrations of Rb, Ba, U, Th, and K and low contents of HFSE (Fig. 5). Our collection included no samples with geochemical features typical of adakites (high LREE/HREE ratios) (Fig. 6).

The transverse zoning in the distribution of trace elements is well pronounced. The anomalously low (<1) normalized Nb and Ta concentrations in the frontal-zone volcanics increase to 2 MORB values in the rear-arc rocks. The K-, Nb-, and Ta-enriched rear-arc rocks have relatively high concentrations of HREE and LREE, Rb, Ba, U, and Th at high LREE/HREE ratios (Fig. 7). Weakly pronounced Eu anomalies are discernible only in the patterns of lavas

Concentrations of major (wt %) and trace (ppm) elements and radiogenic isotopes in representative samples of volcanic rocks from the Kuril island arc

Component	KY-72/73	KY-108/73	KY-P1-2002	KY-@-4	KY-@-2	KY-Al-1	KY-1470	KY-08
	1	2	3	4	5	6	7	8
	Kunashir Isl. (F)			Iturup Isl. (F)				Iturup Isl. (R)
SiO_2	52.45	52.87	51.93	52.15	55.49	49.56	50.04	51.79
TiO_2	1.16	1.18	1.10	0.73	0.82	0.38	0.80	0.92
Al_2O_3	16.52	16.18	16.38	16.46	16.73	12.32	18.54	20.53
Fe_2O_3	12.53	12.60	12.88	10.48	10.17	9.88	12.08	9.04
MnO	0.21	0.21	0.18	0.18	0.25	0.20	0.20	0.20
MgO	4.52	4.52	5.21	7.80	4.18	11.15	5.00	3.42
CaO	9.27	9.26	9.30	9.46	8.97	14.58	10.68	9.68
Na_2O	2.98	2.90	2.80	2.28	2.53	0.70	2.13	3.25
K_2O	0.66	0.67	0.60	0.48	0.63	0.07	0.23	0.61
P_2O_5	0.18	0.19	0.23	0.18	0.19	0.02	0.06	0.26
Total	100.48	100.58	100.61	100.2	99.96	98.86	99.76	99.7
Rb	13.53	12.42	11.80	7.06	10.12	2.24	1.32	8.31
Ba	198.60	253.10	196.20	147.70	209.90	18.30	35.45	94.20
Pb	6.66	6.39	6.52	5.69	5.85	2.00	1.90	5.91
Zr	93.16	90.85	87.07	47.44	50.41	10.17	16.52	47.74
Hf	2.59	2.55	2.29	1.46	2.06	0.38	0.76	1.85
La	5.40	6.11	5.56	3.16	3.54	0.91	1.23	4.47
Ce	15.17	16.59	15.33	7.33	9.61	1.61		10.56
Pr	2.52	2.42	2.33	1.24	1.40	0.39	0.52	1.99
Nd	13.37	12.72	11.68	5.81	7.08	1.84	2.65	9.54
Sm	4.09	3.83	3.59	1.97	2.14	0.89	0.98	3.05
Eu	1.24	1.19	1.14	0.74	0.82	0.34	0.44	1.15
Gd	3.41	3.39	4.60	1.66	2.01	0.75	0.83	2.51
Tb	0.89	0.91	0.77	0.51	0.59	0.29	0.29	0.76
Dy	5.88	5.46	5.15	3.27	3.77	1.79	1.88	4.41
Ho	1.15	1.15	1.09	0.69	0.81	0.39	0.40	0.92
Er	3.19	3.35	2.94	2.00	2.28	1.11	1.16	2.53
Tm	0.47	0.47	0.45	0.30	0.38	0.17	0.18	0.38
Yb	3.35	3.22	3.04	2.03	2.44	1.10	1.23	2.62
Lu	0.47	0.50	0.45	0.31	0.37	0.17	0.20	0.40
Nb	1.20	1.12	1.16	0.48	0.57	0.10	0.28	0.84
Y	29.80	27.19	29.37	18.44	21.25	9.91	7.54	20.81
Ta	0.09	0.08	0.08	0.04	0.05	0.01	0.02	0.06
Th	1.20	1.02	1.02	0.53	0.78	0.08	0.21	0.68
U	0.40	0.39	0.37	0.23	0.30	0.03	0.10	0.25
Be	0.49	0.47	0.50	0.24	0.28	0.07	0.18	0.44
$^{87}Sr/^{86}Sr$	0.703238	0.703273	0.703177	0.703236	0.703269	0.703297	0.703465	0.703352
$^{143}Nd/^{144}Nd$	0.513042	0.513041	0.513095	0.513062	0.513021		0.513000	0.513060
$^{206}Pb/^{204}Pb$	18.39	18.39	18.371	18.345	18.397	18.401	18.504	18.387
$^{207}Pb/^{204}Pb$	15.529	15.52	15.525	15.538	15.533	15.543	15.516	15.527
$^{208}Pb/^{204}Pb$	38.23	38.23	38.233	38.252	38.277	38.305	38.240	38.253

Table. (Contd.)

Component	KY-233/84	KY-20/76	KY-191/84	KY-229/83	KY-26/83	KY-56/84	KY-10/84	KY-11/84
	9	10	11	12	13	14	15	16
	Chernye Brat'ya Isls. (F)	Boutona Isl. (R)	Simushir Isl. (F)				Rasshua Isl. (F)	
SiO_2	52.62	54.04	54.14	52.12	54.96	52.24	55.88	51.50
TiO_2	0.72	0.72	1.02	0.83	0.80	0.72	0.60	0.60
Al_2O_3	18.50	17.14	17.82	18.33	17.50	18.75	16.63	16.60
Fe_2O_3	9.69	6.53	10.94	10.33	9.79	9.32	8.43	10.66
MnO	0.17	0.14	0.19	0.16	0.16	0.19	0.16	0.21
MgO	4.97	7.13	3.26	5.45	3.98	5.30	5.30	6.17
CaO	9.96	9.22	8.36	9.35	8.69	9.62	6.62	9.28
Na_2O	2.92	2.64	3.38	2.85	3.06	2.60	3.12	2.55
K_2O	0.63	1.89	0.76	0.48	0.54	0.30	1.50	0.77
P_2O_5	0.13	0.28	0.17	0.16	0.18	0.15	0.08	0.13
Total	100.31	99.73	100.04	100.06	99.66	99.19	98.32	98.47
Rb	9.32	29.15	11.32	8.60	8.43	18.94	18.44	12.35
Ba	189.90	214.50	135.80	120.20	151.80	68.89	349.30	140.70
Pb	4.92	28.37	4.78	5.17	3.71	2.56	10.01	6.61
Zr	74.65	84.79	86.72	47.65	56.82	47.84	66.14	53.36
Hf	1.54	2.56	2.52	1.51	1.54	1.49	2.62	1.58
La	5.64	13.23	5.91	3.39	4.71	3.11	5.34	3.23
Ce	13.06	33.94	15.55	8.85	12.64	8.82	13.79	8.64
Pr	1.82	3.53	2.22	1.33	1.87	1.45	2.05	1.33
Nd	9.81	16.22	11.62	6.70	9.30	7.91	10.19	6.93
Sm	2.62	3.69	3.26	2.16	2.76	2.50	3.10	2.22
Eu	0.92	1.38	1.20	0.79	0.97	0.95	0.93	0.78
Gd	2.25	3.61	2.93	2.71	3.41	3.25	3.84	2.94
Tb	0.61	0.75	0.82	0.48	0.60	0.57	0.68	0.52
Dy	3.54	4.13	5.23	3.23	4.01	3.84	4.60	3.51
Ho	0.69	0.69	0.95	0.71	0.86	0.82	1.01	0.76
Er	2.04	2.17	2.81	1.98	2.40	2.29	2.83	2.13
Tm	0.31	0.31	0.44	0.32	0.37	0.35	0.44	0.34
Yb	2.14	2.02	2.94	2.11	2.58	2.34	3.10	2.23
Lu	0.31	0.32	0.46	0.33	0.39	0.37	0.47	0.35
Nb	1.08	3.13	1.46	0.89	1.28	0.77	1.05	0.65
Y	18.00	17.91	26.09	20.45	19.92	22.23	25.41	19.98
Ta	0.08	0.20	0.11	0.08	0.09	0.06	0.09	0.06
Th	0.96	3.23	1.21	0.64	0.72	0.38	1.41	0.70
U	0.35	1.06	0.45	0.27	0.24	0.17	0.59	0.32
Be	0.43	0.76	0.53	0.40	0.48	0.35	0.47	0.34
$^{87}Sr/^{86}Sr$	0.703155	0.702993	0.703271	0.703213	0.703283	0.703003	0.703413	0.703617
$^{143}Nd/^{144}Nd$	0.513017	0.513058	0.513136	0.513158	0.513171	0.513063	0.513129	0.513179
$^{206}Pb/^{204}Pb$	18.397	18.021	18.409	18.395	18.384	18.373	18.430	18.450539
$^{207}Pb/^{204}Pb$	15.523	15.576	15.527	15.523	15.537	15.511	15.534	15.564336
$^{208}Pb/^{204}Pb$	38.234	38.109	38.251	38.231	38.257	38.172	38.294	38.365115

Table. (Contd.)

Component	KY-36/76	KY-1301	KY-46/72	KY-41/72	KY-47/72	KY-34/72	KY-161/72
	17	18	19	20	21	22	23
	Matua Isl. (F)	Paramushir Isl. (F)				Atlasovo Isl. (R)	
SiO_2	55.31	52.40	52.98	58.81	54.90	49.01	48.91
TiO_2	0.84	0.72	0.74	0.67	0.68	0.92	0.80
Al_2O_3	18.08	20.75	16.30	16.72	15.51	19.68	20.77
Fe_2O_3	9.09	8.67	10.12	8.22	9.79	10.72	8.85
MnO	0.16	0.17	0.17	0.18	0.18	0.17	0.17
MgO	3.41	3.90	7.50	3.00	4.98	3.78	4.91
CaO	8.45	9.46	8.10	7.00	8.23	10.78	10.54
Na_2O	3.15	2.84	2.65	3.00	3.14	2.85	2.83
K_2O	0.96	1.03	1.40	2.17	1.90	1.61	1.65
P_2O_5	0.25	0.08	0.27	0.18	0.22	0.35	0.36
Total	99.7	100.02	100.23	99.95	99.53	99.87	99.79
Rb	14.13	14.45	30.62	78.12	35.91	32.82	43.70
Ba	183.30	227.90	323.30	2098.00	252.80	158.90	
Pb	7.25	8.96	6.22	8.09		4.19	4.69
Zr	53.24	52.78	68.25	102.50	82.22	63.95	115.10
Hf	2.00	1.72	2.30	2.96	2.25	1.89	2.02
La	7.80	6.47	9.51	11.74	9.76	11.28	12.94
Ce	18.54	16.64	22.06	28.78	23.27	24.96	33.47
Pr	2.73	2.32	3.14	3.52	3.16	3.53	3.83
Nd	13.26	10.68	14.01	16.10	14.23	15.31	19.26
Sm	3.54	2.99	3.50	3.62	3.50	3.88	4.30
Eu	1.19	1.07	1.08	1.04	1.04	1.29	1.38
Gd	3.86	2.98	3.32	3.85	3.49	3.82	4.26
Tb	0.62	0.60	0.59	0.58	0.54	0.59	0.61
Dy	3.99	3.75	3.61	3.77	3.47	3.49	3.87
Ho	0.83	0.76	0.73	0.77	0.71	0.72	0.75
Er	2.36	2.21	2.11	2.17	2.04	1.94	2.11
Tm	0.37	0.34	0.31	0.35	0.32	0.31	0.32
Yb	2.52	2.25	2.20	2.45	2.15	1.95	2.12
Lu	0.39	0.35	0.33	0.39	0.34	0.31	0.31
Nb	1.36	1.19	1.66	2.05	1.73	3.66	3.35
Y	21.06	20.54	18.67	21.55	19.24	18.74	21.50
Ta	0.08	0.08	0.35	0.14	0.11	0.22	0.20
Th	1.40	1.30	2.76	4.09	2.74	2.14	2.29
U	0.49	0.46	1.01	1.49	1.01	0.78	0.90
Be	0.55	0.48	0.64	0.69	0.67	0.86	0.84
$^{87}Sr/^{86}Sr$	0.703141	0.703225	0.703245	0.703271	0.703174	0.703186	0.703044
$^{143}Nd/^{144}Nd$	0.513129	0.513100	0.513106	0.513072	0.513072	0.513106	0.513027
$^{206}Pb/^{204}Pb$	18.422	18.053	18.447	18.446	18.412	18.503	18.467
$^{207}Pb/^{204}Pb$	15.539	15.536	15.511	15.510	15.523	15.512	15.512
$^{208}Pb/^{204}Pb$	38.311	38.040	38.222	38.222	38.218	38.240	38.211

Note: (*1–3*) Tyatya volcano; (*4*) Men'shoi Brat volcano; (*6*) Kudryavyi volcano; (*7*) L'vinaya Past' volcano; (*8*) Bogdan Khmel'nitskii volcano; (*9*) Brat Chirpoev volcano; (*10*) Broutona volcano; (*11–13*) Uratman volcano; (*14*) Prevo volcano; (*15*, *16*) Rasshua volcano; (*17*) Sarychev volcano; (*18*) Churachki volcano; (*19–21*) Ebeko volcano; (*22*, *23*) Alaid volcano. F and T are the frontal and rear zones, respectively. The analyses were made at the Shimane University in Matsue, Japan. Major elements were analyzed by XRF; trace elements were determined by ICP-MS on a Thermo ELEMENTAL VG PQ3; radiogenic isotopes were analyzed on a Finnigan MAT 262 thermal-ionization mass spectrometer (TIMS).

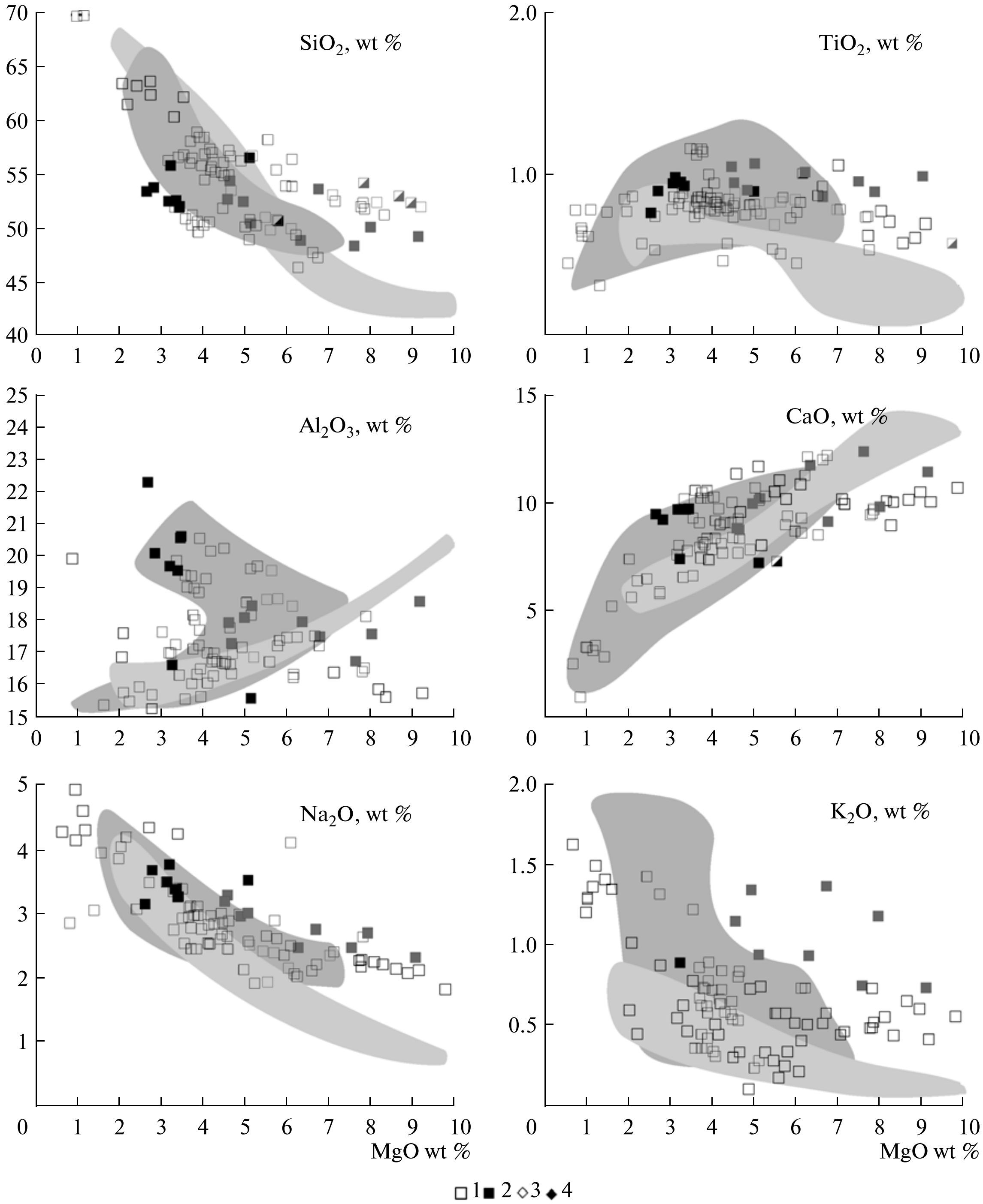

Fig. 2. Variations in the concentrations of major elements in Quaternary lavas from the southern and northern islands of the Kuril arc depending on the MgO concentrations.

(*1, 2*) Iturup Island: (*1*) frontal and (*2*) rear zones; (*3, 4*) islands: (*3*) Paramushir (frontal zone) and (*4*) Atlasovo (rear zone). Fields show the compositions of lavas from the frontal (pale gray) and rear (gray) zones of Kunashir Island.

Here and below, gray symbols show data from (Frolova et al., 1985).

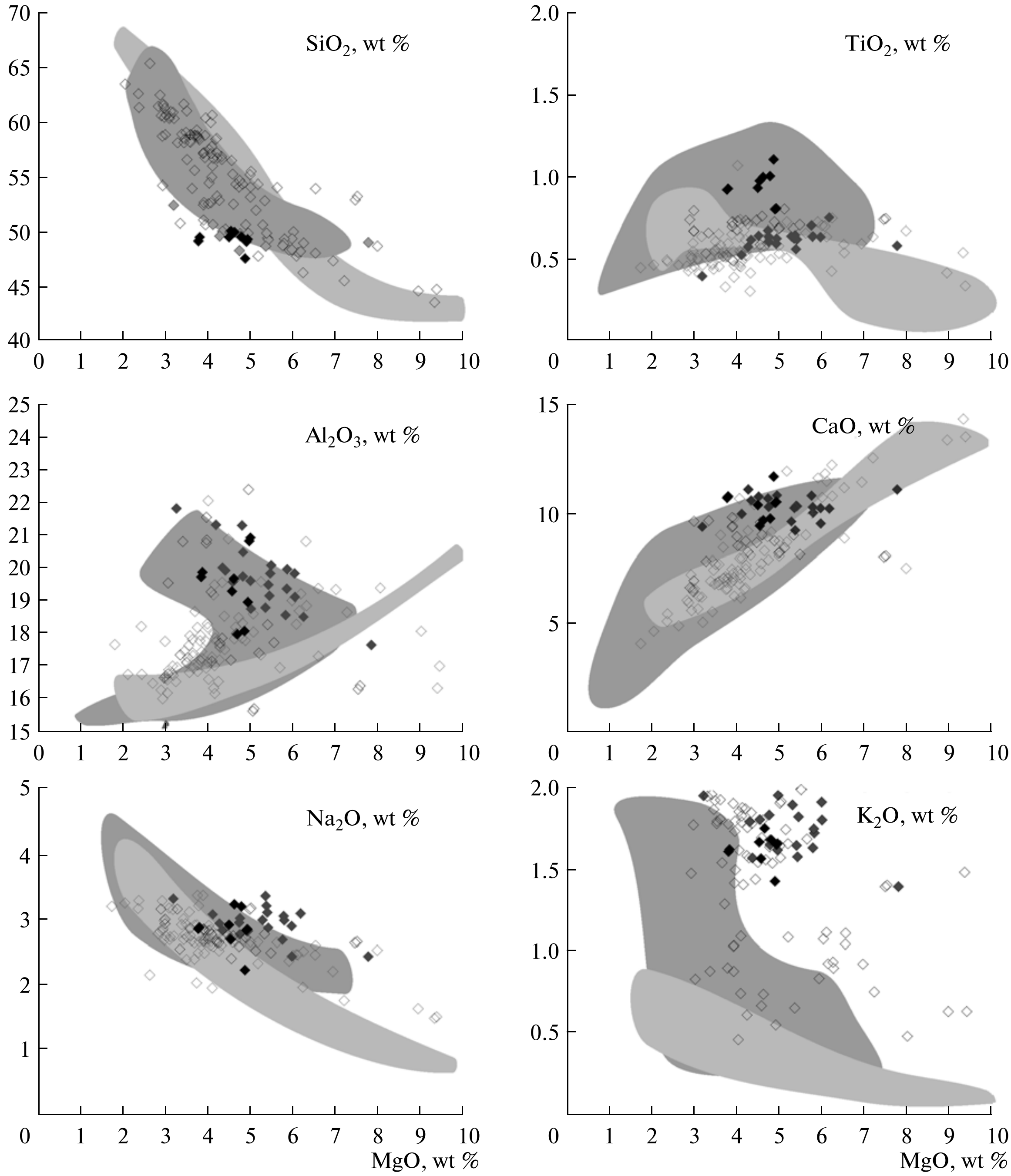

Fig. 2. Contd.

from Kunashir Island, and none of our samples showed Ce anomalies.

A longitudinal geochemical zoning is most clearly pronounced in the frontal zone. Modern basalts in the islands of Kunashir and Iturup are depleted in LREE (Fig. 7) and are noted for anomalously low normalized concentrations of Nb and Ta (Fig. 5). With regard for the low Na_2O and K_2O concentrations, this testifies to a depleted composition of the parental magmas. The front-arc volcanics in the central and, particularly, northern Kuril Islands are enriched in LREE.

Analogous relations and tendencies, although pronounced not as clearly, are also typical of the rear-arc lavas, whose LREE/HREE ratios systematically increase northward (Fig. 7).

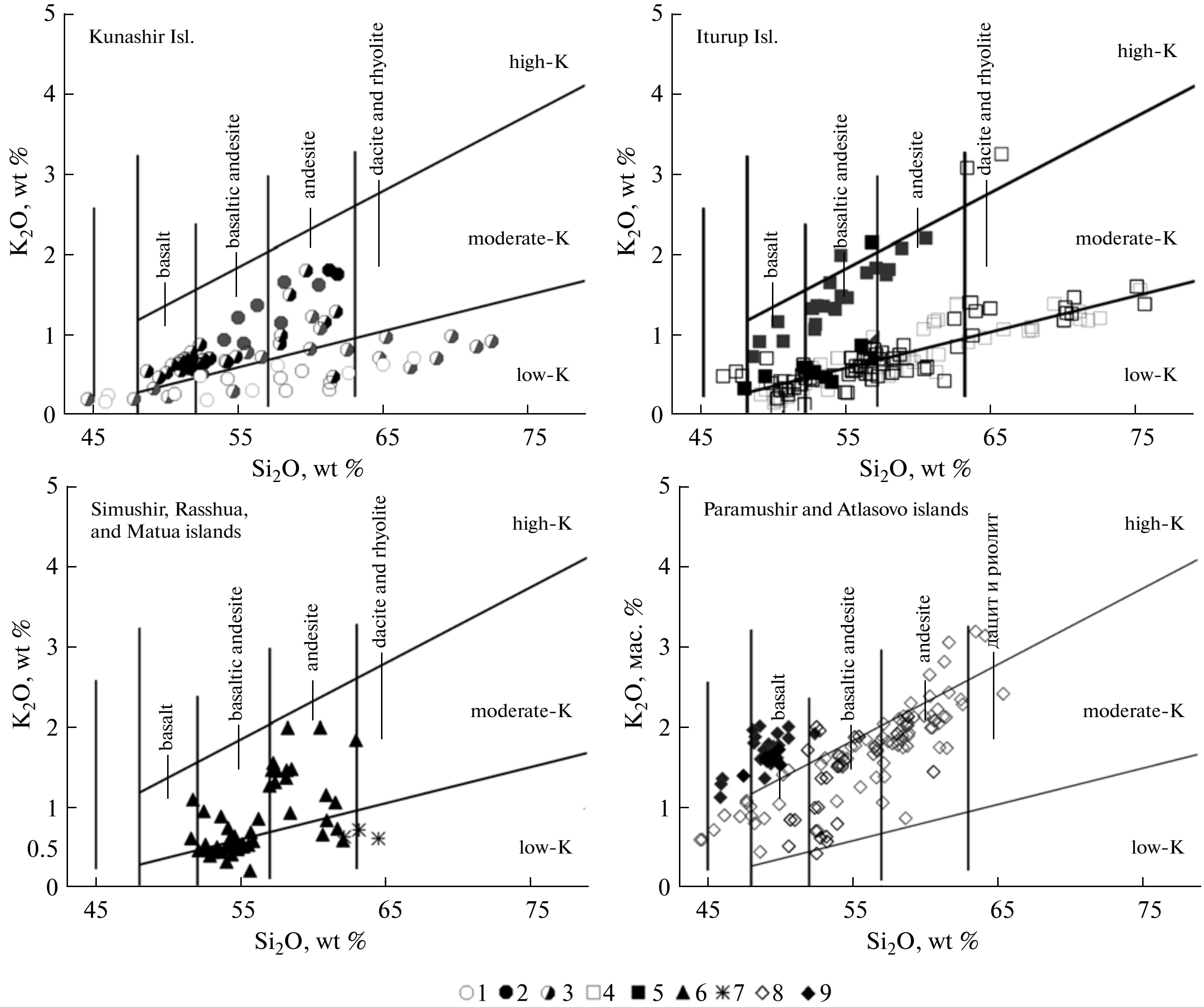

Fig. 3. SiO_2-K_2O classification diagram for Quaternary lavas in the Kuril Islands.
(*1, 2*) Kunashir Island: (*1*) frontal and (*2*) rear zones; (*3*) Tyatya volcano with transitional geochemical characteristics; (*4–*) Iturup Island: (*4*) frontal and (*5*) rear zones; (*6*) Simushir Island; (*7*) Rasshua and Matua islands; (*8*) Paramushir Island; (*9*) Atlasova Island.

Radiogenic Isotopes

The volcanics of the Kuril island arc are characterized by narrower variations in the Sr, Nd, and Pb isotopic ratios than those in rocks from many other island arcs, including the Japanese arc. In the isotope diagrams of Figs. 8–10, our samples plot within compact fields between the fields of Quaternary volcanic rocks in Kamchatka and Japan.

A transverse geochemical zoning is clearly pronounced in the $^{143}Nd/^{144}Nd$ and $^{87}Sr/^{86}Sr$ isotopic ratios (Fig. 8). The rear-arc lavas and the rocks of submarine volcanoes lie within the compositional fields of MORB in the Indian Ocean. The only exceptions are two samples whose isotopic characteristics are close to those of the frontal-arc volcanics. One of these samples (sample KY-08) was taken from the bottom part of Bogdan Khmelnitskii volcano (Iturup Island), and the other one (sample KY-34/72) is from the vicinity of the summit of Alaid volcano (Atlasovo Island). The latter sample is interesting in that it characterizes a marginal zone of a modern (still hot) lava flow. The frontal-arc basalts and andesites are noted for higher concentrations of radiogenic Sr and, often, Nd (Fig. 8). The $^{87}Sr/^{86}Sr$ isotopic ratios practically do not vary along the arc strike (0.703145–0.703297). The only exceptions are two samples of basalt from the central zone (samples KY 10/84 and KY 11/84) with higher concentrations of radiogenic Sr (table, Fig. 8), perhaps, because of contamination with seawater.

In contrast to the $^{87}Sr/^{86}Sr$ ratio, the $^{143}Nd/^{144}Nd$ isotopic ratio of the frontal-arc rocks varies within broader range (table, Fig. 8). Lavas from the southern (Kunashir, Iturup, and Chernye Brat'ya) sector are

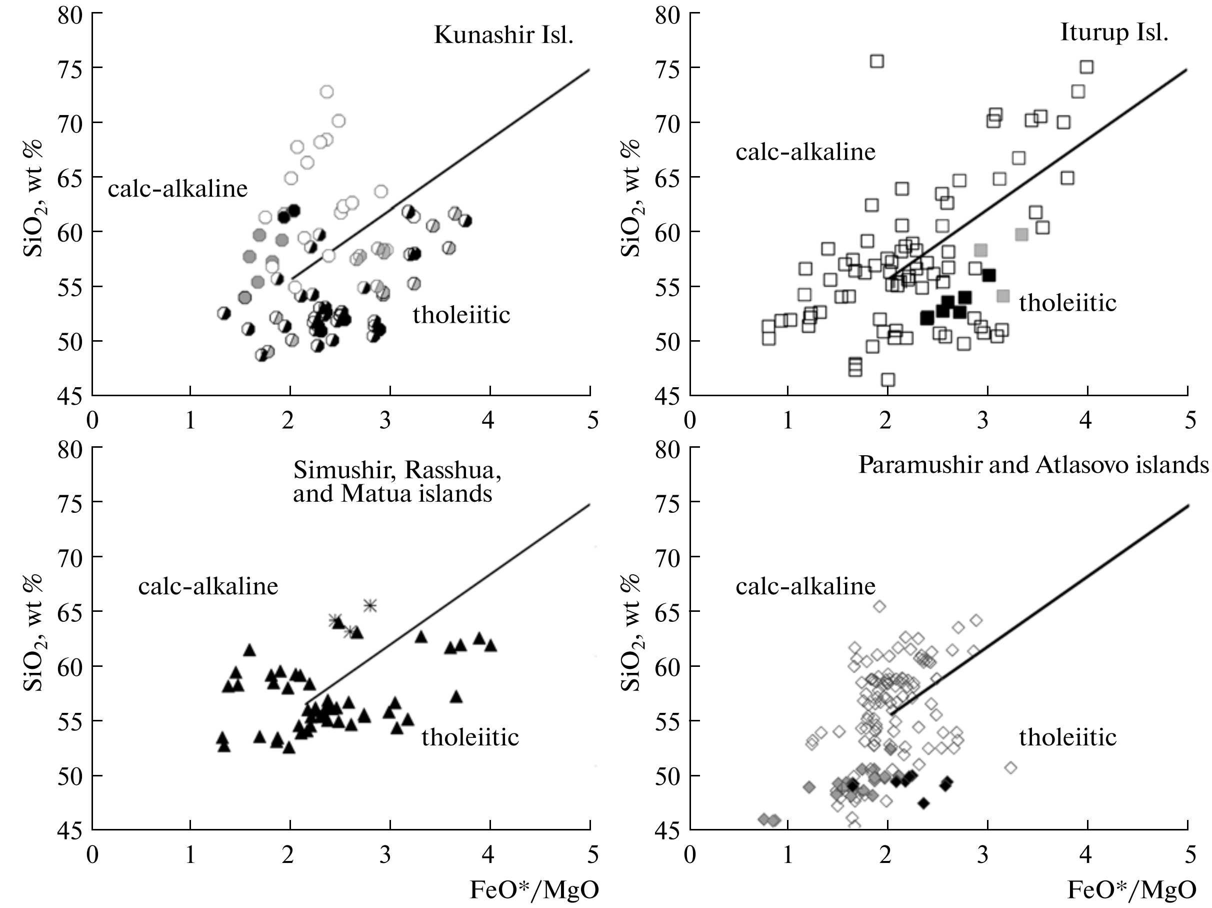

Fig. 4. SiO_2-FeO*/MgO diagram
See Fig. 3 for symbol explanations.

less radiogenic, and those from the central and northern sectors are more radiogenic. Data presented in (Zhuravlev et al., 1985) corroborate these conclusions: only two of the 24 samples plot away from the aforementioned trend.

In Pb isotopic diagrams (Figs. 9, 10), all of our samples lie within the field of MORB in the Indian Ocean and plot between the compositions of Quaternary lavas in Kamchatka and Japan. The lowest $^{207}Pb/^{204}Pb$ and $^{208}Pb/^{204}Pb$ and the highest $^{206}Pb/^{204}Pb$ ratios were detected in lavas from the islands of Paramushir and Atlasovo. Analogous features are shown by samples dredged from submarine volcanoes (Avdeiko et al., 2009) in the rear zone of the southern group of the Kuril Islands (Figs. 9, 10).

DISCUSSION

Similarities between the principal geological and geodynamic parameters of the subduction process throughout the whole Kuril island arc, including the thicknesses of the continental crust, the age and slope of the downgoing oceanic slab, and the depths of the Benioff zone, suggest that magmatic processes should also have been similar throughout the arc. This is, however, in conflict with geodynamic and geochemical data. With regard for the volcanic genesis of the islands, their different surface areas (Fig. 1) led us to suggest that the magma-generating system had a variable productivity, which was anomalously high at the flanks of the volcanic arc. Geochemical variations of the magmatic products along the strike of the arc suggest variations in the magma generation parameters.

Crustal Contamination

Crustal contamination is often though to make an important contribution to the compositional variations of arc magmatic rocks (Gill, 1981; Kersting et al., 1996). For example, systematic variations in the isotopic-geochemical characteristics of Quaternary lavas in the frontal zone of northeastern Japan are thought (Kimura and Yoshida, 2006) to be related to differences in the composition of the contaminating melts.

Although the Kuril Islands were formed on a continental basement, interaction processes with crustal material likely did not play any significant role in

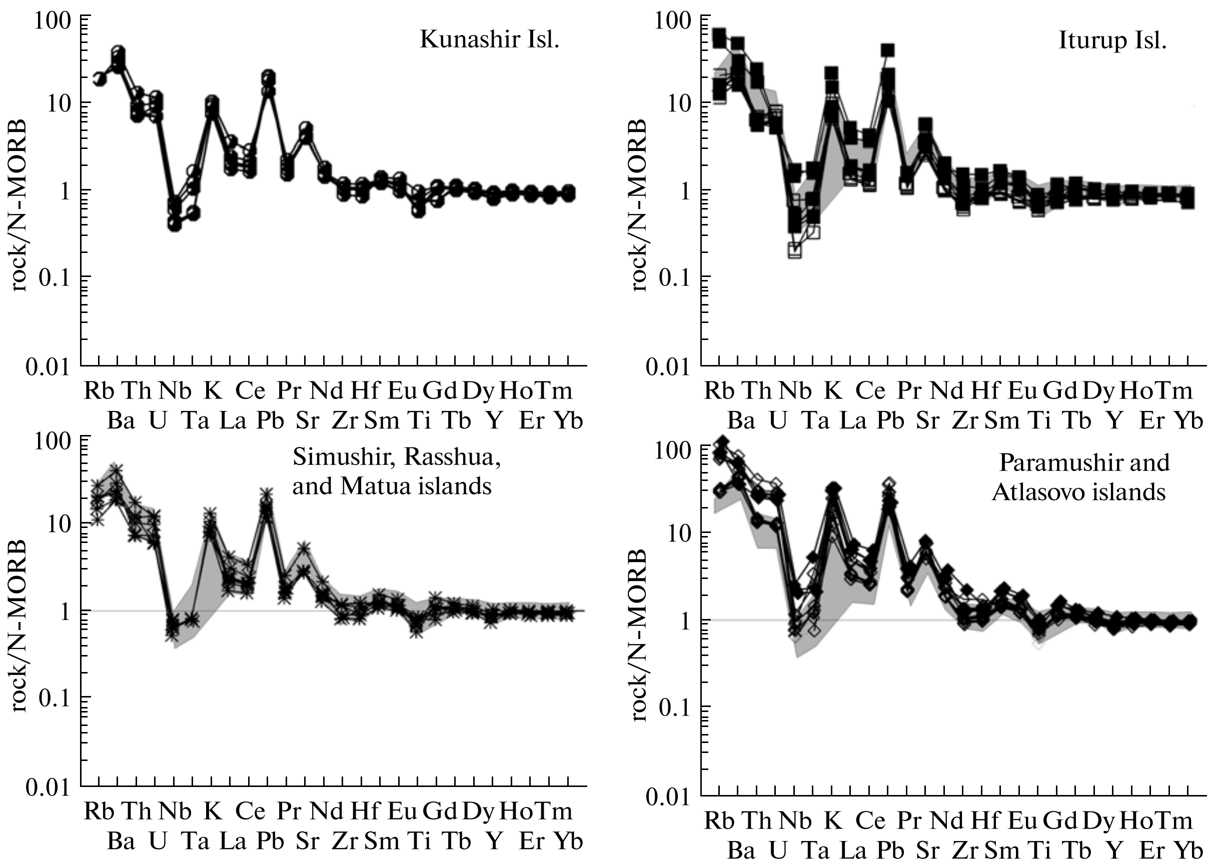

Fig. 5. N-MORB-normalized trace-element patterns of basalts from the Kuril Islands
See Fig. 3 for symbol explanations. The gray field corresponds to Quaternary lavas from Tyatya volcano, Kunashir Island.

magma generation (Ryan et al., 1995; Martynov et al., 2010). In the $^{143}Nd/^{144}Nd$–SiO_2 diagram (Fig. 11), Quaternary lavas from the volcanic front and rear zone define a subvertical trend with insignificant variations in the SiO_2 concentrations, which could result from either the isotopic heterogeneity of the suprasubduction mantle or the mixing of melts from enriched and depleted mantle sources. The latter mechanism was suggested in (Shuto et al., 2004) to explain the variations in the isotopic characteristics of basalts in Hokkaido as the age of the rocks becomes younger. Crystallization differentiation corresponds to a subhorizontal trend, and the fractionation of crystals associated with crustal contamination are portrayed as a diagonal trend (*AFC* trend in Fig. 11).

An insignificant role of crustal contamination in the magma generation of modern mafic and intermediate lavas of Gorelyi and Mutnovskii volcanoes in southern Kamchatka, which are situated in the vicinity of the northern termination of the Kuril arc system, was mentioned in (Duggen et al., 2007). This also follows from the subhorizontal trend for rocks of the two volcanic edifices in the $^{143}Nd/^{144}Nd$–SiO_2 diagram (Fig. 11).

Isotopic heterogeneity of the suprasubduction mantle. Because of the masking effect of subduction components, it is fairly hard to evaluate the composition of the suprasubduction mantle (Elliot, 2003). The concentration of radiogenic Sr is largely controlled by the fluid phase, and the $^{143}Nd/^{144}Nd$, $^{206}Pb/^{204}Pb$, $^{207}Pb/^{204}Pb$, and $^{208}Pb/^{204}Pb$ ratios are determined by the subduction sediment, whose Pb and Nd concentrations are roughly one order of magnitude higher than the corresponding mantle values.

Nevertheless, the general trends of the lateral variations in the isotopic characteristics of Quaternary volcanics in the Kuril Islands suggest that the mantle source was isotopically heterogeneous. In this context, the most illustrative diagram is $^{208}Pb/^{204}Pb$–$^{206}Pb/^{204}Pb$ (Fig. 10), in which volcanic rocks from the northern sector, on the one hand, and from the southern and central ones, on the other, define discrete but subparallel trends. The former are characterized by relatively low $^{208}Pb/^{204}Pb$ ratios close to those of lavas in southern Kamchatka. The data points of mafic volcanics from the northern sector plot slightly above the line for the average compositions of Pacific MORB (NHRL). The compositions of Quaternary volcanics of the southern and central islands shift toward the more radiogenic region of MORB in the Indian Ocean and partly overlap the fields of modern volcanics in the Japanese arc system. These variations do not coincide with the calculated mixing lines for the depleted mantle and subducted sediment (Fig. 10) and suggest that the composition of the suprasubduction mantle wedge was isotopically heterogeneous.

The variations in the Nd isotopic characteristics of the analyzed samples (Fig. 8) can be approximated by a model for the mixing of suprasubduction mantle and sedimentary material. However, similarities between the lavas in the southern Kuril islands and Japan and between the lavas in Paramushir Island and in Kamchatka can be more logically explained, with regard for Pb isotopic data, by the involvement of mantle domains (of the enriched Indian-Ocean MORB type in the south and depleted, close to Pacific MORB, in the north) in the course of the melting process.

The heterogeneity of the suprasubduction mantle has already been documented in long arc structures, such as the Tonga–Kermadec arc system (Turner et al., 1997), and was suggested for the Japanese system (Arculus, 1994).

Degree of Melting of the Mantle Source

Possessing depleted isotopic characteristics, the basalts of Paramushir Island are enriched in K_2O, HFSE, and LREE, conceivably, as a result of a relatively low-degree of melting of the magmatic source. This hypothesis is, however, not corroborated by either geological or geochemical lines of evidence. Paramushir is the second largest island in the Kuril island arc, and this testifies to a high productivity of the magmatic system. Moreover, the high-K Quaternary lavas of this island are characterized by low TiO_2 concentrations. Although the bulk Ti distribution coefficients for the mineral assemblage of the peridotite mantle are much higher than the K distribution coefficients (~0.2 and ~0.01, respectively; Langmuir et al., 1992; Kelemen et al., 1993), both elements are incompatible and should have been enriched in the early portions of the melt, which is, however, not the case.

Subduction-Related Components

Elevated K_2O concentrations in lavas from Paramushir Island (Fig. 3) can be explained by the involvement of sedimentary material in the magma generation processes, with this material significantly enriched in this component compared to basalts of the MORB type, which are typical derivatives of the depleted mantle. This model is confirmed by distinctive features in the behavior of the elements.

Volcanic rocks from the frontal zone of the southern Kurils are enriched in elements mobile in aqueous chloride solutions, such as Ba, U, and Cs (Brenan et al., 1995). In Fig. 12, the data points of our samples are prone to plot near a subvertical trend, and this suggests that an important role in their genesis was played by a subduction fluid generated by the partial dehydration of modified oceanic crustal material and/or sediment. In contrast to this, the compositions of volcanics from Paramushir Island obviously shift toward high Th/Yb ratios and define a subhorizontal trend. With regard for its high concentrations in oceanic sediments (Fig. 12) and low bulk distribution coefficients in the sediment–melt system (Plank and Langmuir, 1998; Jhonson and Plank, 1999), Th is an important indicator of the involvement of melting products of sediments in magma-generating processes. Note that the insignificant differences between the Th/Yb ratios of the suprasubduction sediments in the southern and northern Kurils cannot explain why the volcanics define different trends, as was hypothesized in (Bailey, 1996; Ishikawa and Tera, 1997).

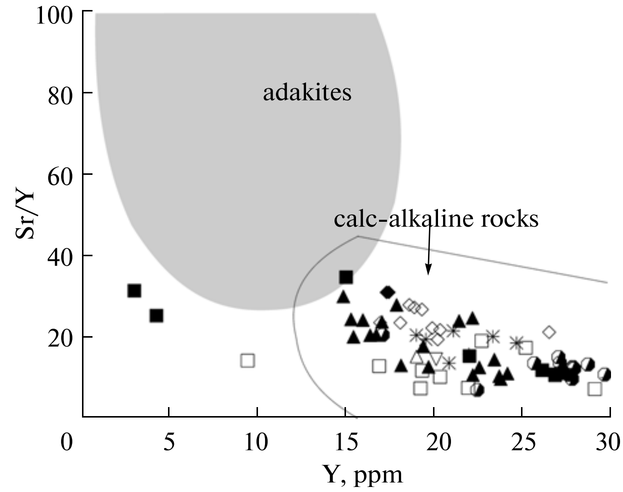

Fig. 6. Sr/Y-Y classification diagram (Defant and Drummond, 1990).
See Fig. 3 for symbol explanations.

An analogous situation occurs with the rear-arc volcanics. For example, basalts in the rear zone of Iturup Island (Bogdan Khmelnitskii volcano) have low Th/Yb ratios, which are close to those in the frontal-arc lavas (Fig. 12). The eruption products of the northernmost volcano Alaid in the rear zone and of Geofizikov volcano in the Kuril Basin (Baranov et al., 2002) have Th/Yb = 0.9–1.7. The maximum values (1.5–2.7) of this ratio were detected in the arc basalts of Broutona Island on the boundary between the southern and central sectors.

The Yb–Th diagram in Fig. 13 shows, along with the data points of the Kuril lavas, also the calculated compositions of the fluid phase (700°C) and melt (800°C) that are generated at, respectively, the dehydration and melting of sedimentary material. The bulk composition of the sedimentary sequence subducted beneath the southern and northern Kurils is compiled from (Plank and Langmuir, 1998), and the Th and Tb distribution coefficients between the sediment, fluid,

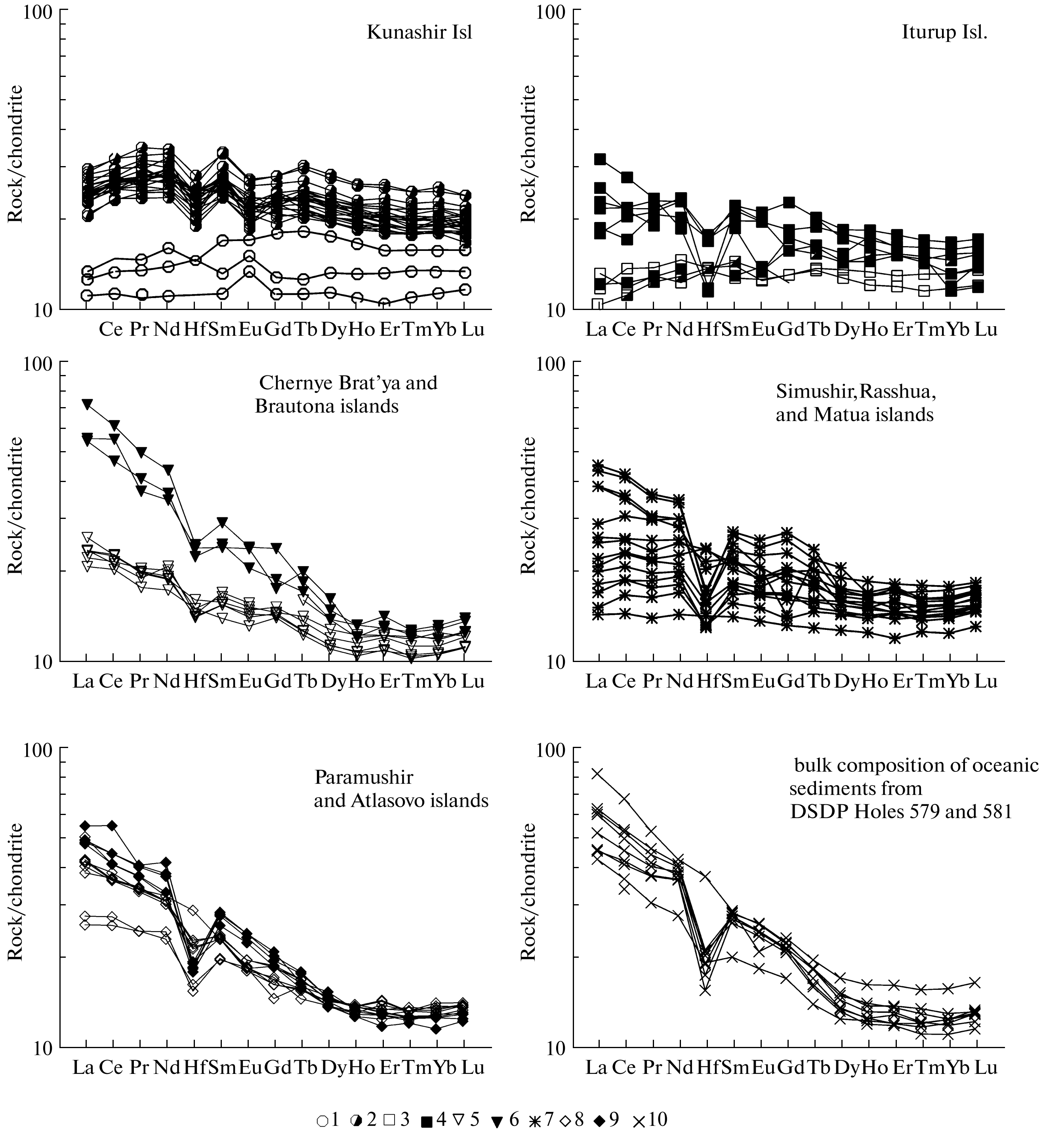

Fig. 7. Chondrite-normalized REE and Hf patterns of Quaternary lavas from the Kuril island arc.
(*1, 2*) Kunashir Island: (*1*) frontal and (*2*) rear zones; (*3, 4*) Iturup Island: (*3*) frontal and (*4*) rear zones; (*5, 6*) Chernye Brat'ya islands, (*5*) frontal zone, (*6*) Broutona Island, rear zone; (*7*) Simushir, Matua, and Rasshua islands, central zone; (*8*) Paramushir Island; (*9*) Atlasovo Island; (*10*) average composition *Fo* oceanic sediments recovered by DSDP Holes 579 and 581 (Plank and Langmuir, 1998). Note that negative Hf anomalies are most clearly pronounced in volcanic rocks with high REE concentrations and LREE/HREE ratios.

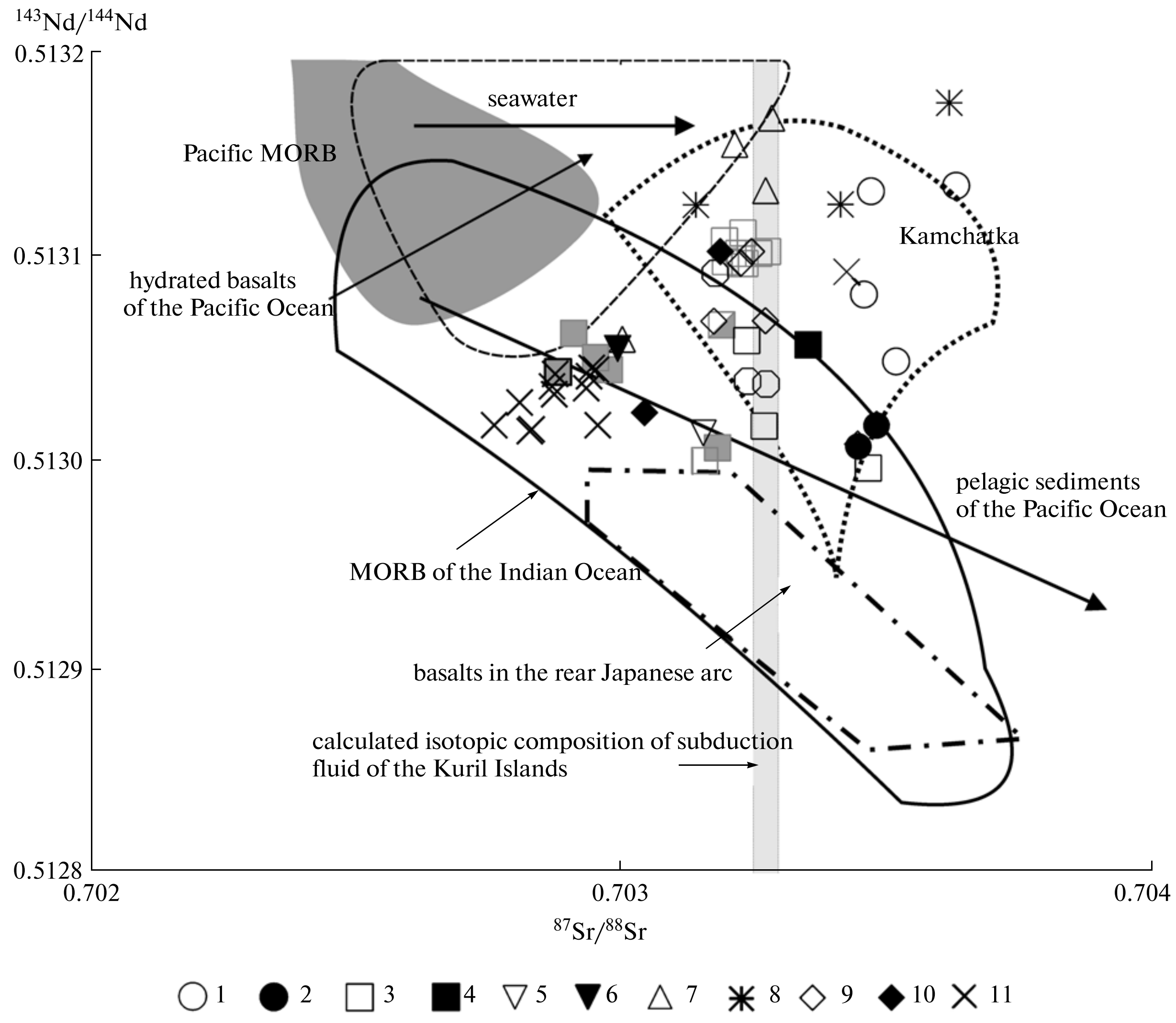

Fig. 8. Sr and Nd isotopic ratios of Quaternary lavas from the Kuril island arc.

(*1, 2*) Kunashir Island: (*1*) frontal and (*2*) rear zones; (*3, 4*) Iturup Island: (*3*) frontal and (*4*) rear zones; (*5, 6*) Chernye Brat'ya islands, (*5*) frontal zone, (*6*) Broutona Island, rear zone; (*7*) Simushir Island; (*8*) Rasshua and Matua islands; (*9*) Paramushir Island; (*10*) Atlasovo Island; (*11*) submarine volcanoes of the Kuril Basin (Baranov et al., 2002; Bindeman and Bailey, 1999).

Gray symbols are data from (Zhuravlev et al., 1985). The isotopic composition of the subduction fluid of the Kurils was calculated based on (Ishikawa and Tera, 1977).

Compositional fields: basalts of the Pacific Ocean (gray), basalts of the Indian Ocean (solid-line contour), hydrated oceanic basalts (dashed line), Quaternary volcanics of Kamchatka dotted line), basalts from the rear Japanese arc (dash-and-dot line).

and melt are from (Jhnson and Plank, 1999). The diagonal trend of rocks from the southern islands suggests the predominant influence of a fluid phase, whereas the horizontal trend of the northern islands and rear-arc volcanics implies the predominant effect of melts derived from sediments.

Our conclusions are corroborated by the behavior of Hf in the Kuril lavas. Hf and LREE have similar mineral–melt distribution coefficients and are not fractionation from one another in the course of melting of the unmodified mantle, for example, of the MORB or OIB types. Considering the different solubility of these elements in aqueous chloride solutions, Pearce et al. (1999) suggested that the negative Hf anomalies in arc volcanics are related to subduction-related fluid. However, Hf in the Kuril rocks is correlated with Th, an element indicating that melts were derived via the melting of sedimentary material. The lowest relative concentrations of the element are typical of rear-arc and frontal-arc lavas in the northern sector of the island arc (Fig. 7). The relatively low Hf concentrations of the sedimentary material (Fig. 7) provide grounds to suggest that silicate melt played a determining role in Hf fractionation from LREE.

Figure 14 shows calculated mixing lines for the compositions of modified oceanic crust, fluid, and

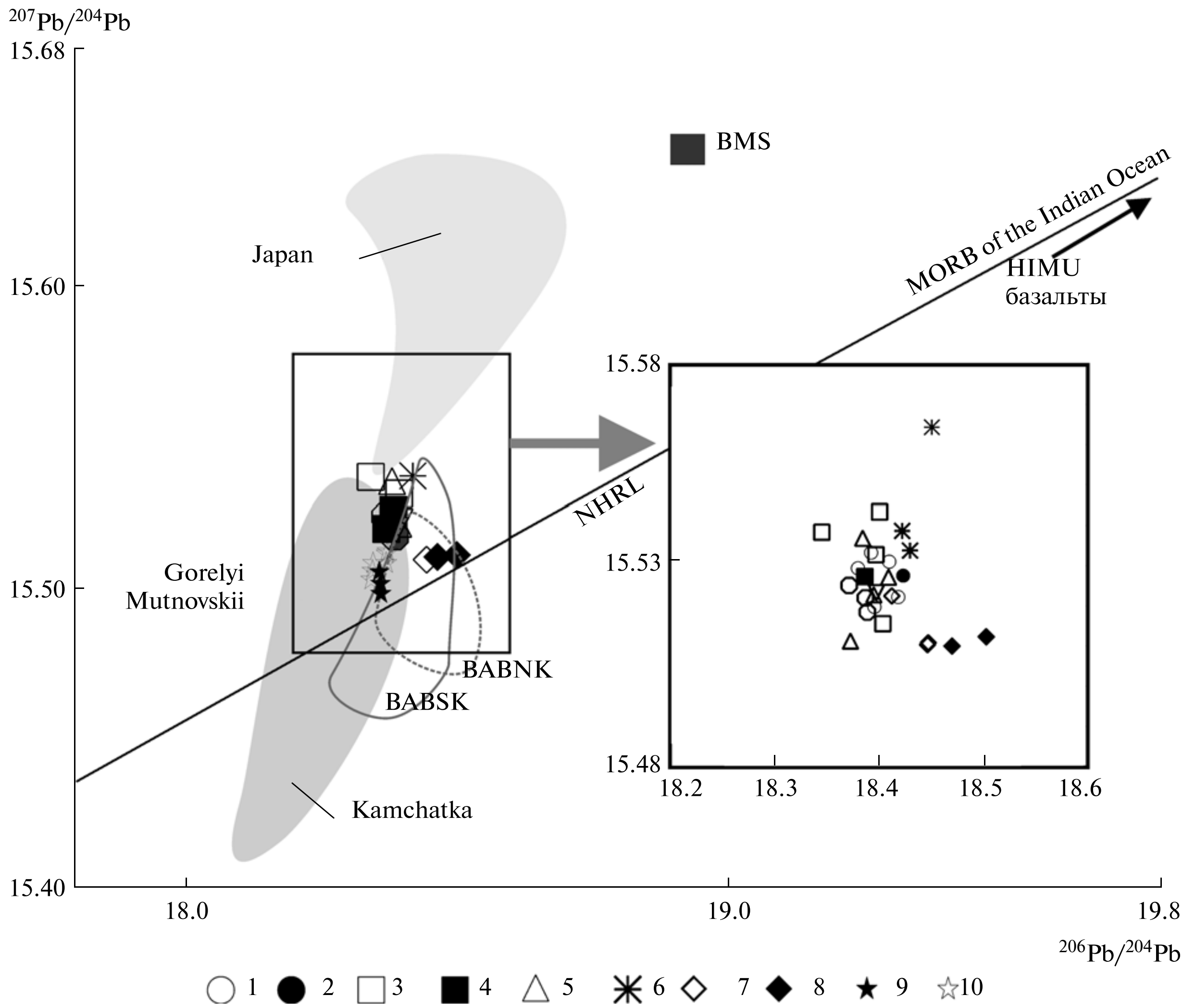

Fig. 9. $^{206}Pb/^{204}Pb$-$^{208}Pb/^{204}Pb$ for Quaternary lavas from the Kuril island arc. The inset shows scaled-up outlined quadrangle. (*1–4*) See Fig. 8; (*5*) Simushir Island; (*6*) Rasshua and Matua islands; (*7*) Paramushir Island; (*8*) Atlasovo Island; (*9, 10*) volcanoes (*9*) Gorelyi and (*10*) Mutnovsklii in southern Kamchatka (Duggen et al., 2007).

Fields show the composition of rear-arc lavas in the northern (dashed line) and southern (solid line) sectors of the Kuril island arc (Avdeiko et al., 2009), Japan, and Kamchatka. *BMS* is the bulk composition of the sediments; *NHRL* (Northern Hemisphere Reference Line) is the line of average basalt composition for the Northern Hemisphere; *HIMU* (High U/Pb) is the hypothetical magmatic source with a high U/Pb ratio; *BABSK* and BABNK are basalts of, respectively, the southern and northern parts of the Kuril Basin.

melt generated by, respectively, the dehydration and melting of sedimentary material subducted beneath the Kuril Islands. The subducted component of basalts in the southern islands is a fluid phase generated mostly by the dehydration of the oceanic crust, which is in good agreement with data in (Ishikawa and Tera, 1997). The magma generation processes of lavas in the northern islands were participated, along with a fluid phase, also by a melt derived from sediments (up to ~5%).

Geochemical features of the melting of sediments beneath the northern Kurils and the absence of rocks with adakite features (Fig. 6) testify that the surface of the subducted oceanic slab was relatively hot (~650–800°C), and its temperature was higher than the water-saturated solidus temperature of oceanic sediments but lower than the temperature at which the melting of modified oceanic crustal material begins (>800°C) (Poli and Schmidt, 2002). In this respect, the northern Kuril Islands are closely similar to the Aleutian and Mariana arc systems in the Central American active margin (Class et al., 2000; George et al., 2003; and others).

Similar relations were also detected in the modern lavas of Gorelyi and Mutnovskii volcanoes in southern Kamchatka (Duggen et al., 2007). An important role of melts related to the melting of sedimentary material is thought by these authors to result from the relatively

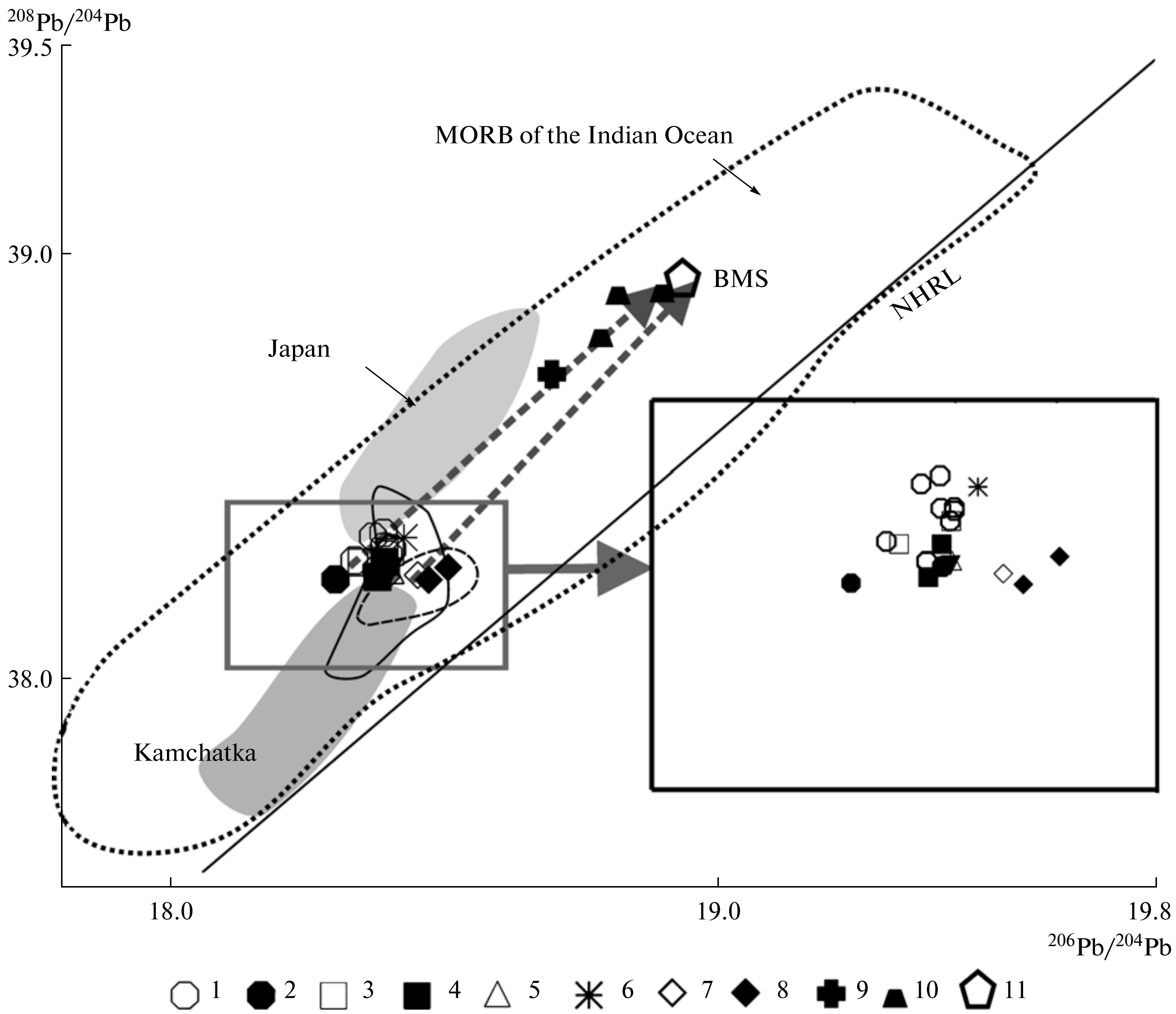

Fig. 10. $^{208}Pb/^{204}Pb$-$^{206}Pb/^{204}Pb$ diagram for lavas from the Kuril Islands. The inset shows scaled-up outlined quadrangle. (*1–8*) Same as in Fig. 9; (*9, 10*) average composition of subducted sediment in (*9*) the Mariana and (*10*) Kuril-Kamchatka island arcs; (*11*) bulk composition of oceanic sediments (Plank and Langmuir, 1998). Lines contour the following fields: rear-arc lavas of the northern (dashed line) and southern (solid line) sectors of the Kuril island arc (Avdeiko et al., 2009) and *MORB* of the Indian Ocean (dashed line). The gray field corresponds to Quaternary lavas in Japan and Kamchatka. Gray dashed-line arrows are calculated mixing lines for partial mantle melts and sedimentary material.

high mantle temperatures, and this finds support in data on melt inclusions in the mantle rocks (~1275°C at a pressure of ~1.5 GPa) and results of thermal simulations for geophysical parameters (Manea et al., 2005). If the Kamchatka thermal anomaly resulted from the heating of the downgoing oceanic slab by a mantle plume beneath Guyot Meiji (Manea and Manea, 2008), it is reasonable to suggest that it extends southward, into the region of the southern islands of the Kuril arc.

Many researchers believe that southern Kamchatka is the northerly continuation of the structures of the Kuril island arc. However, with regard for isotopic and geochemical data, it seems to be more accurate and reasonable to admit the opposite: structural elements of southern Kamchatka extend southward into the territory of the northern Kuril Islands.

The relatively high role of melts derived by the melting of sedimentary material is also identified in the rear-arc basalts of the central and northern Kuril Islands and submarine Geofizikov volcano (Kirile Basin), and this is generally consistent with earlier data (Ryan et al., 1995; Morris and Ryan, 2003), which were based, for example, on the ^{10}Be distribution. Analogous relations in the change from fluid subduction component in the frontal zone to melt derived from sediments in the rear zone was demonstrated in (Plank and Kelley, 2001) for the Izu arc. High temperatures at the surface of the subducted slab in the rear zone can be explained by either the significant depths at which the magmatic melts are formed (see, for

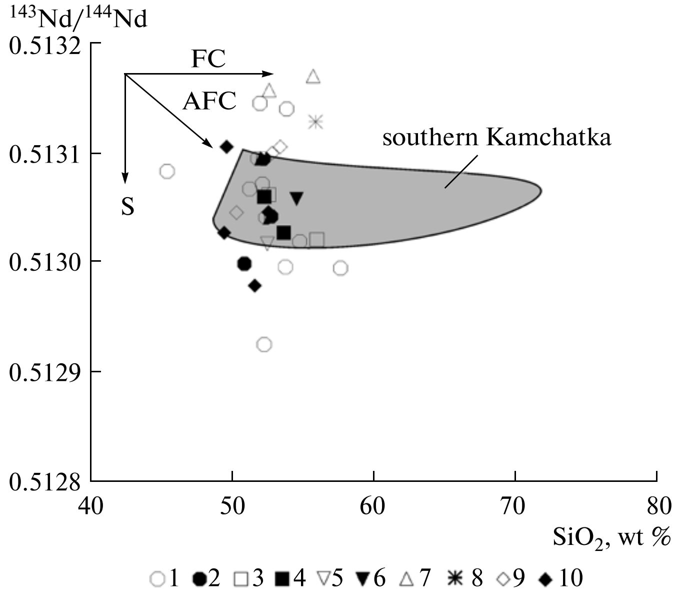

Fig. 11. $^{143}Nd/^{144}Nd$-SiO_2 diagram for volcanic rocks from the Kuril Islands (modified after Martynov et al., 2010).
(*1, 2*) Kunashir Island: (*1*) frontal and (*2*) rear zones; (*3, 4*) Iturup Island: (*3*) frontal and (*4*) rear zones; (*5, 6*) Chernye Brat'ya islands, (*5*) frontal zone, (*6*) Broutona Island, rear zone; (*7*) Simushir Island; (*8*) Rasshua and Matua islands; (*9*) Paramushir Island; (*10*) Atlasovo Island.
The solid line contours the compositional field of lavas from Gorelyi and Mutnovskii volcanoes (Duggen et al., 2007); *FC* is fractional crystallization, *ACF* is crystallization differentiation and crustal contamination, *S* is variations in the compositions of the source.

example, Morris and Ryan, 2003) or the unusual thermal regime due to the activity of backarc tectono-magmatic processes.

Role of Backarc Tectono-Magmatic Processes

Geochemical features of suprasubduction volcanic rocks often suggest their mantle source that is more strongly depleted in incompatible elements even compared to the source of depleted oceanic basalts of the N-MORB type. This is traditionally explained by the effect of earlier magmatic events in the rear zone, the opening of the backarc basin, and the displacement of depleted mantle domains to the volcanic front by convective motions (McCulloch and Gamble, 1991; Woodhead et al., 1993; Turner et al., 1997; and others).

The composition the suprasubduction mantle had before it was modified by subduction processes can be evaluated from the concentrations and proportions of so-called conservative incompatible elements, which are characterized by low concentrations in the subducted sediment and aqueous fluid (Woodhead et al., 1993; and others). Major components least susceptible to the effect of subduction are Na_2O and TiO_2. For example, the concentrations of these elements in the sedimentary material subducted beneath the northern and southern Kuril Islands are either much lower than (for TiO_2) or close to (for Na_2O) those in N-MORB (table).

The trace element indicators most commonly utilized for these purpose are ratios of HFSE (Ta, Nb, Zr, and Hf) (Pearce and Parkinson, 1993; Davvidson et al., 1996; and others), highly incompatible elements with similar bulk mineral–melt distribution coefficients, which are not fractionated from one another even in relatively highly aqueous environments. For example, the Nb/Ta ratio in melt practically does not change in the presence of magnesian amphibole (Tiepolo et al., 2000). In the absence of garnet in the residue assemblage, one of the most conservative elements in subduction environments is Yb (Pearce et al., 2004). The Sm/La ratio is often used as an indicator of a mantle source (Plank, 2005). Although La is more incompatible than Sm, these differences should not lead to any significant variations in the Sm/La ratio in magmas derived at relatively high degrees of melting typical of island arc systems.

The Na_8–Fe_8 diagram in Fig. 15 shows the compositions of the Kuril lavas (MgO > 5 wt %) normalized to 8 wt % MgO. Anomalously low Na_2O concentrations characterize the Quaternary basalt of Kunashir Island (Martynov et al., 2005), whose data points lie in the upper part of the field of experimental partial melts derived from depleted peridotite (Na_8 < 1.8 wt %) (Fig. 15). Relatively low normalized Na_2O concentrations are typical of mafic volcanics from Iturup Island and islands in the central sector. Basalts from Paramushir, the northernmost island, have high potassic alkalinity and are the only ones that plot near the main

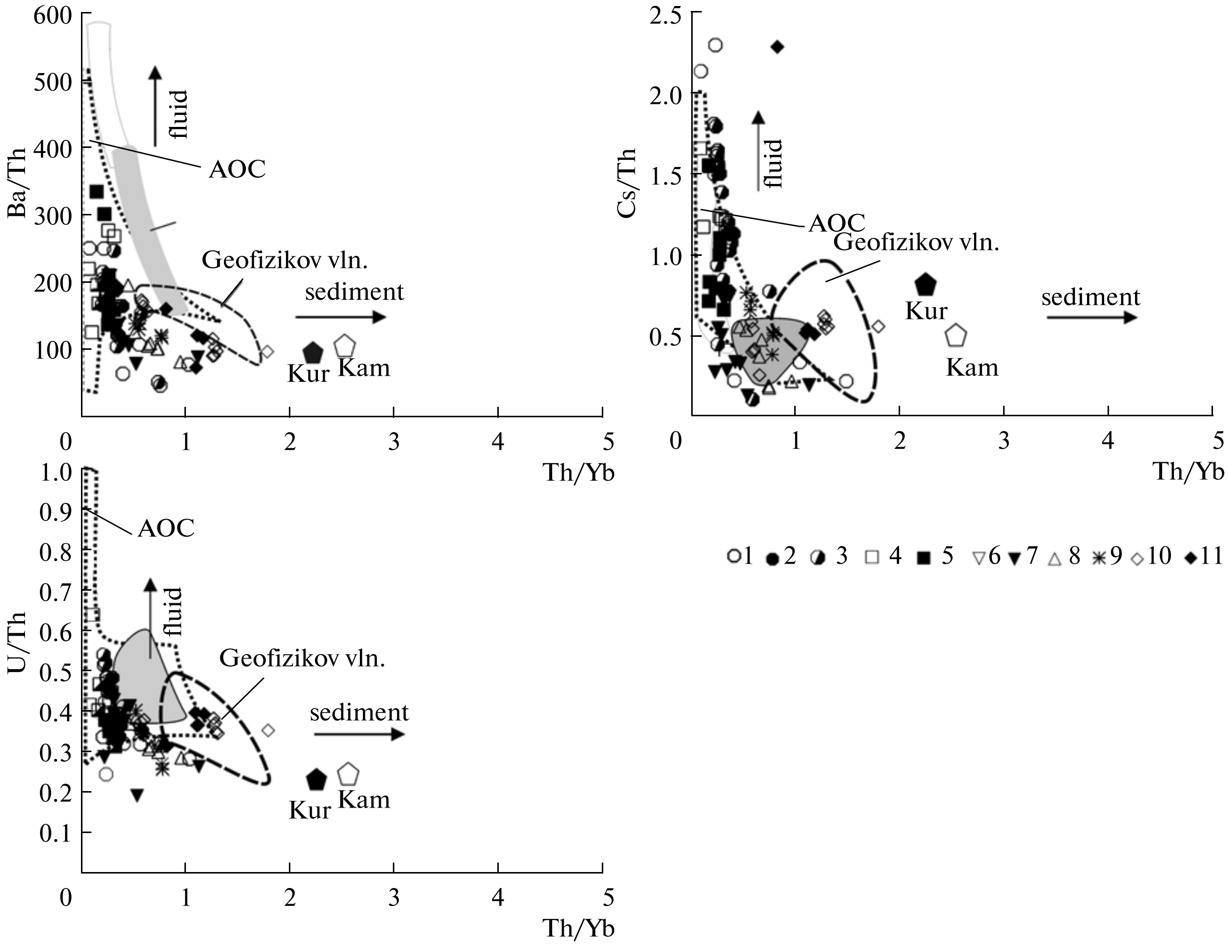

Fig. 12. Ba/Th-Th/Yb, Cs/Th-Th-Yb, and U/Th-Th/Yb diagrams for Quaternary volcanic rocks from the Kuril island arc. (*1, 2*) Kunashir Island: (*1*) frontal and (*2*) rear zones; (*3*) Tyatya volcano; (*4, 5*) Iturup Island: (*4*) frontal and (*5*) rear zones; (*6*) Chernye Brat'ya islands; (*7*) Broutona Island; (*8*) Simushir Island; (*9*) Rasshua and Matua islands; (*10*) Paramushir Island; (*11*) Atlasovo Island.

The diagrams show the average composition of sediments subducted beneath the Kuril (*Kur*) and Kamchatka (*Kam*) segments of the island arc (Plank and Langmuir, 1998). Composition *Fo* volcanic rocks: Geofizikov submarine volcano (dashed line) (Baranov et al., 2002), altered ocean crust *AOC* (dotted line), Mutnovskii volcano (thin solid line), and Gorelyi volcano (gray field) (Duggen et al., 2007).

trend of oceanic basalts and can be regarded as derived from enriched peridotite.

The depleted character of basalts from the two southern islands is consistent with trace-element data. Figure 16 shows variations in the Nb/Yb and Zr/Hf ratios of mafic lavas in the Kuril island arc. The Nb/Yb ratio of the frontal-arc basalts from islands of the northern and central sectors vary near the average values typical of N-MORB (~0.8), whereas these ratios of rocks from Kunashir and Iturup islands are 0.3–0.08. The Zr/Hf ratio is also remarkably lower than the chondritic one, with these data considered together confirming that magma-generating processes beneath the southern islands involved depleted mantle material. Considering that depletion in trace elements does not affect the isotopic characteristics of the rocks and is directly correlated with the degree of opening of the Kuril backarc basin, it is reasonable to suggest that the composition of the mantle source of the lavas was affected by relatively young back-arc tectono-magmatic events. The direct correlation of the geochemical characteristics of the magmas with the intensity of backarc processes was previously documented in the Tonga–Kermadec arc (Turner et al., 1997).

Transverse Geochemical Zoning

Because of the limited number of the analyzed samples, we do not touch here upon the genesis of the transverse geochemical zoning of the Kuril island arc, and the conclusion presented below should be regarded as tentative.

Although geochemical data suggest that the role of melts whose genesis is related to the melting of sub-

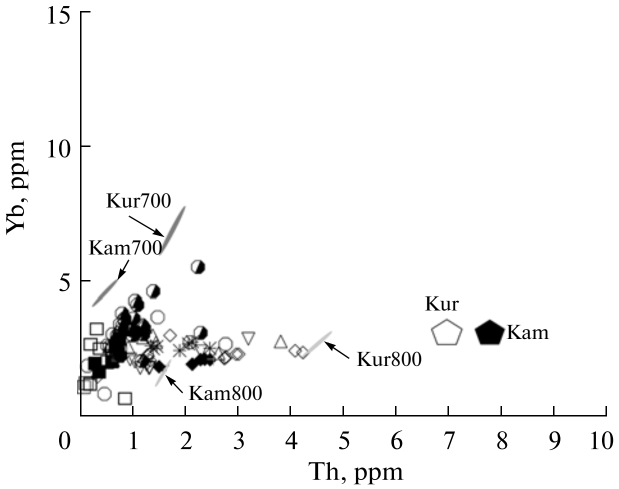

Fig. 13. Yb-Th diagram for Quaternary lavas from the Kuril Islands.

See Fig. 12 for symbol explanations. The diagram shows calculated compositions of the fluid phase (700°C) and melt (800°C) generated at, respectively, the dehydration and melting of sediments subducted beneath the Kamchatka (*Kam*) and Kuril (*Kur*) segments of the island arc system. The average composition of the sedimentary sequence is according to (Plank and Langmuir, 1998); the bulk distribution coefficients of elements in the sediment/melt system are according to (Jhonson and Plank, 2002).

It can be clearly seen that compositional variations of volcanic rocks from the southern Kuril Islands were controlled by a low-temperature fluid phase, and those of rocks from the northern Kuril Islands were controlled by melt derived via the melting of sedimentary material.

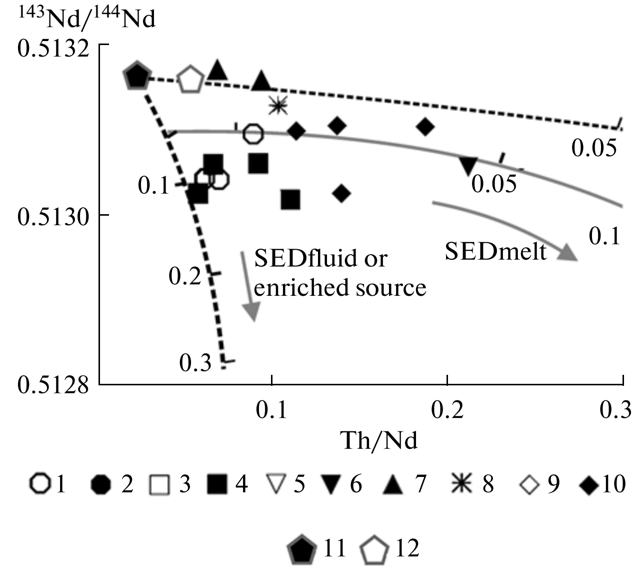

Fig. 14. $^{143}Nd/^{144}Nd$-Th/Nd diagram for the Quaternary lavas.

(*1, 2*) Kunashir Island: (*1*) frontal and (*2*) rear zones; (*3, 4*) Iturup Island: (*3*) frontal and (*4*) rear zones; (*5, 6*) Chernye Brat'ya islands, (*5*) frontal zone, (*6*) Broutona Island, rear zone; (*7*) Simushir Island; (*8*) Rasshua and Matua islands; (*9*) Paramushir Island; (*10*) Atlasovo Island; (*11*) basalts of the altered oceanic crust (*AOC*); (*12*) calculated composition of AOC fluid. The diagram does not show data on all of the zones and islands. The diagram shows calculated mixing lines for AOC basalts with melt (*SEDmelt*) and a fluid phase (*SEDfluid*) formed by, respectively the melting and dehydration of subducted sediments. In the calculations, the composition of the sediments was assumed to correspond to the average composition of the sedimentary sequence subducted beneath the Kuril island arc (Plank and Langmuir, 1998); the bulk distribution coefficients are compiled from (Jhonson and Plank, 2002): 700°C for the fluid phase and 800°C for the melt.

ducted sediments increases in the magma-generating processes in the rear zone, this process cannot account for the specifics of the distribution of radiogenic isotopes in volcanics of the Kuril arc system. The behavior of Sr and Nd isotopes in our samples is largely close to that in Quaternary lavas in northeastern Japan (Kimura and Yoshida, 2006). The rear-arc basalts display homogeneous enough isotopic characteristics and define a compact swarm in the field of MORB of the Indian Ocean, whereas mafic lavas of the volcanic front are enriched in radiogenic Sr at significant variations in the concentrations of radiogenic Nd. Geochemical simulations led Japanese researchers to conclude that the compositions of the magmatic sources of the frontal- and rear-zone basaltoids were close and that their trace-element and isotopic differences were controlled by the degree of melting and the composition of the crustal contaminant. Inasmuch as neither mineralogical nor geochemical lines of evidence confirm the action of contamination processes in the Kuril island arc, the significant variations in the isotopic characteristics of the lavas across the strike of the arc likely testify to differences in the magmatic sources. Hence, our data are generally consistent with the hypotheses put forth in (*Submarine Volcanism...*, 1992; Bindeman and bailey, 1999).

Similar relations were noted in the Izu–Bonin island arc, in which isotopic–geochemical data suggest the mixing of two mantle sources: slab material from the Philippine Sea in the rear zone and the Pacific oceanic material in the frontal zone (Ishizuka et al., 2003).

Tectonic Zoning

The Kuril island arc is traditionally subdivided into three sectors: southern, central, and northern (Fig. 1). Our data indicate that it would be more accurate to distinguish only two zones (Fig. 17). The northern zone is part of the southern Kamchatka lithospheric block, which has relatively high temperatures and shows depleted isotopic characteristics close to those of the mantle of Pacific MORB. The southern zone is underlain by lithosphere mantle material enriched in

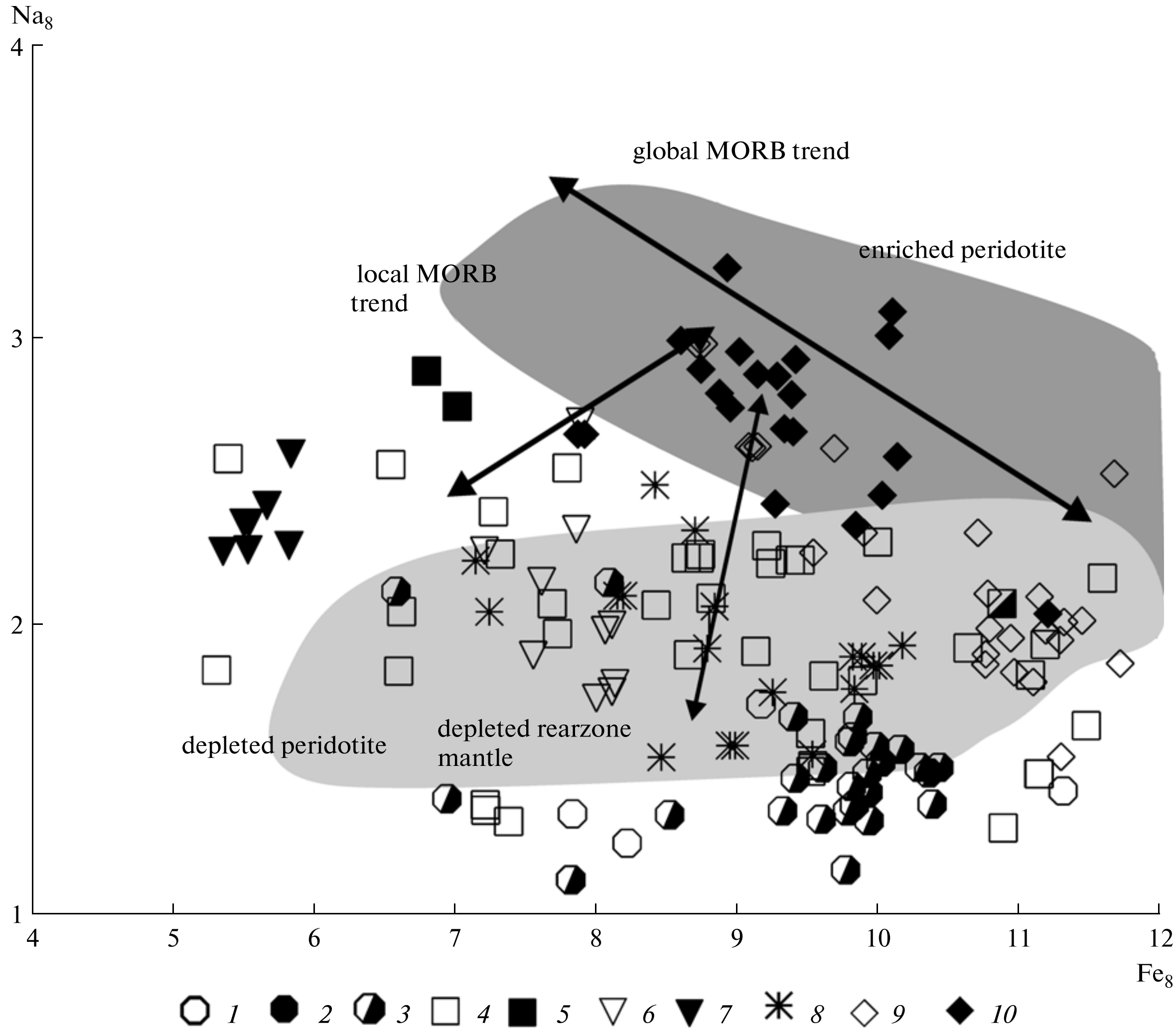

Fig. 15. Variations in the Na_2O and FeO* concentrations in basalts from the Kuril island arc normalized to 8 wt % MgO. Fields and trends are according to (Pearce et al., 1995, with minor modifications).

(*1, 3*) Kunashir Island: (*1*) frontal and (*2*) rear zones and Tyatya volcano; (*4, 5*) Iturup Island: (*4*) frontal and (*5*) rear zones; (*6*) Chernye Brat'ya islands; (*7*) Broutona Island; (*8*) Simushir Island; (*9*) Paramushir Island; (*10*) Atlasovo Island.

Fields show the composition of experimental partial melts derived from depleted (pale gray) and enriched (gray) peridotite (Turner et al., 1997).

The diagram is based on data on samples with SiO_2 concentrations of <54 wt %, LOI < 0.5 wt %, and MgO > 5 wt %.

radiogenic isotopes (MORB of the Indian Ocean) and depleted in trace elements during relatively young magmatic events, likely related to the active opening phase of the Kuril backarc basin. A boundary between these two lithospheric blocks should be drawn somewhere between Matua and Shiashkotan islands. The influence of the temperature anomaly of the Kamchatka Peninsula enhances northward, while the role of processes related to the opening of the Kuril Basin increases southward.

CONCLUSIONS

1. The anomalous geochemical characteristics of volcanic rocks in the northern Kuril islands provide evidence of a high temperature of the suprasubduction mantle in southern Kamchatka and of the involvement of melts derived from oceanic sediments in the magma-generating processes.

2. The trace-element depletion of lavas in the two southernmost islands (Kunashir and Iturup) was induced by relatively young magmatic events likely

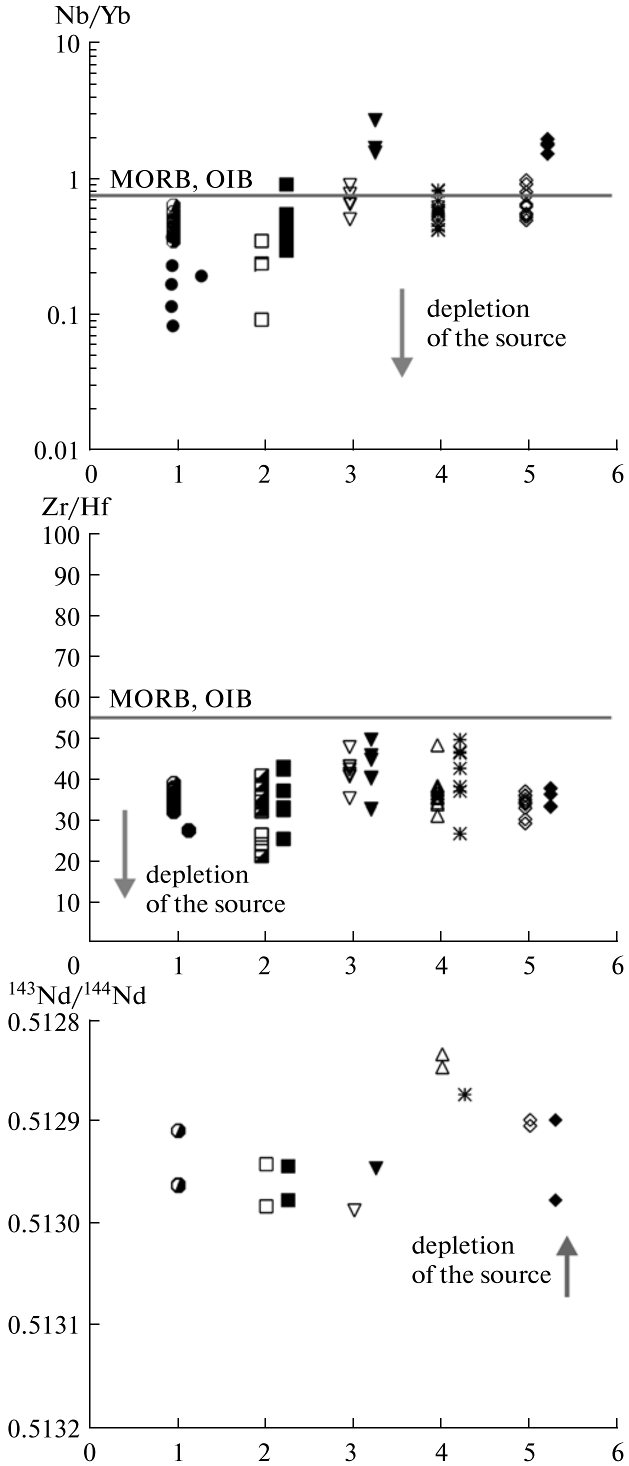

Fig. 16. Variations in the Nb/Yb, Zr/Hf, and $^{143}Nd/^{144}Nd$ ratios in mafic Quaternary lavas in the Kuril island arc.
Numerals along the horizonla axis: (*1*) Kunashir Island; (*2*) Iturup Island; (*3*) Chernye Brat'ya and Broutona islands; (*4*) Simushir and Ketoi islands; (*5*) Paramushir and Atlasovo islands.

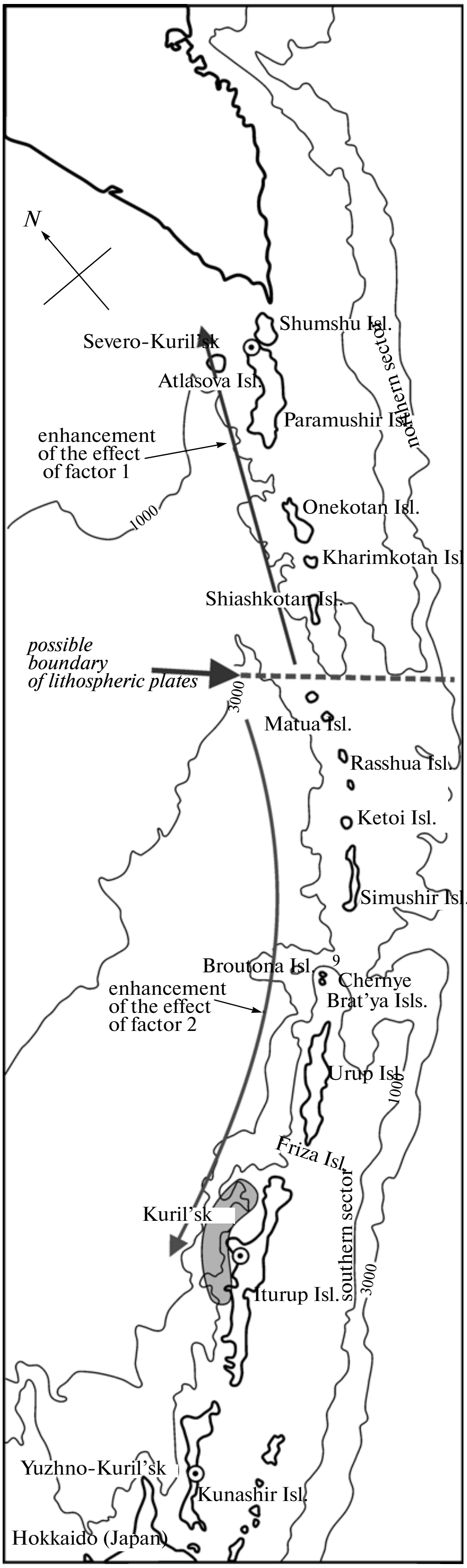

Fig. 17. Tentative tectonic zoning of the Kuril island arc.
Two sectors:
(1) The northern sector develops above the southern Kamchatka lithospheric block, which is hot and isotopically depleted. The northward increase in the size of the islands and, hence, the enhancement of magmatic productivity is controlled by an increase in the temperature of the suprasubduction mantle (factor 1).
(2) The southern sector is underlain by the relatively cold isotopically enriched lithosphere. The systematic southward increase in the size of the islands is related to the increase in the intensity of backarc tectono-magmatic processes during the active opening of the Okhotsk Basin (factor 2).

related to the opening phase of the Kuril backarc basin.

3. The Kuril island arc develops on a heterogeneous basement. Its northern islands rest on the southern Kamchatka lithospheric block, which is relatively depleted and hot. The islands south of them were formed on the cold and isotopically enriched lithospheric mantle, which was depleted in trace elements during relatively young backarc tectono-magmatic processes.

ACKNOWLEDGMENTS

This study was financially supported by the Russian Foundation for Basic Research (project no. 07-05-00310) and projects of the Far East Division, Russian Academy of Sciences (projects nos. 09-11-SO-08-002 and 09-3-A-08-418).

REFERENCES

1. R. J. Arculus, "Aspects of Magma Genesis in Arcs," Lithos **33**, 189-208 (1994).
2. G. P. Avdeiko, S. V. Popruzhenko, and A. A. Palueva, "Modern Tectonic Structure of the Kurile-Kamchatka Region and Conditions of Magma Formation," in *Geodynamics and Volcanism of the Kurile-Kamchatka Island Arc System* (Petropavlovsk-Kamchatskii, 2001), pp. 9-34 [in Russian].
3. G. P. Avdeiko, V. A. Rashidov, A. A. Poluvaeva, and I. M. Romanov, "Subwater Volcanism of the Kurile Range: Geodynamic Conditions and Formation of Geochemical Specifics," http:www.Kscnet.Ru/Ivs/Grant/Grant_06/06-3-A-08-326/index.html
4. J. C. Bailey, "Role of Subducted Sediments in the Genesis of Kuril-Kamchatka Island Arc Basalts: Sr Isotopic and Elemental Evidence," Geochem. J. **30**, 289-321 (1996).
5. J. C. Bailey, T. I. Frolova, and I. A. Burikova, "Mineralogy, Geochemistry and Petrogenesis of Kuril Island-Arc Basalts," Contrib. Minaral. Petrol. **102**, 265 - 280 (1989).
6. B. Baranov, H. K. Wong, K. Dozorova, et al., "Opening Geometry of the Kurile Basin (Okhotsk Sea) as Inferred from Structural Data," The Island Arc **11**, 206-219 (2002).

7. I. N. Bindeman and J. C. Bailey, "Trace Elements in Anorthite Megacrysts from the Kurile Island Arc: A Window to Across-Arc Geochemical Variations in Magma Compositions," Earth Planet. Sci. Lett. **169**, 209-226 (1999).
8. O. A. Bogatikov and A. A. Tsvetkov, *Magmatic Evolution of Island Arcs* (Nauka, Moscow, 1988) [in Russian].
9. J. M. Brenan, H. F. Shaw, F. J. Ryerson, and D. L. Phinney, "Mineral-Aqueous Fluid Partitioning of Trace Elements at 900°C and 2.0 GPa: Constraints on the Trace Elements Chemistry of Mantle and Deep Crustal Fluids," Geochim. Cosmochim. Acta **59**, 3331-3350 (1995).
10. C. Class, D. M. Miller, S. L. Goldstein, and C. H. Langmuir, "Distinguishing Melt and Fluid Subduction Components in Umnak Volcanics, Aleutian Arc," Geochem. Geophys. Geosyst. **1**, GC000010 (2000).
11. J. P. Davidson, "Deciphering Mantle and Crust*al Signatures in Subduction Zone Magmatism," in Subduction: Top to Bottom*, Geophys. Monogr. Am. Geophys. Union **96**, 251-262 (1996).
12. M. J. Defant and M. S. Drummond, "Derivation of Some Modern Arc Magmas by Melting of Young Subducted Lithosphere," Nature **347**, 662-665 (1990).
13. S. Duggen, M. Portnyagin, J. Baker, et al., "Drastic Shift in Lava Geochemistry in the Volcanic-Front to Rear-Arc Region of the Southern Kamchtkan Subduction Zone: Evidence for the Transition from Slab Surface Dehydration to Sediment Melting," Geochim. Cosmochim. Acta **71**, 452-480 (2007).
14. T. Elliot, "Tracers of the Slab," in *Inside the Subduction Factory*, Geophys. Monogr. Am. Geophys. Union **138**, 23-45 (2003).
15. V. I. Fedorchenko, A. I. Abdurakhmanov, and R. I. Rodionova, *Volcanism of the Kurile Island Arc: Geology and Petrogenesis* (Nauka, Moscow, 1989) [in Russian].
16. T. I. Frolova, I. A. Burikova, A. V. Gushchin, et al., *Origin of the Island Arc Volcanic Series* (Nedra, Moscow, 1985) [in Russian].
17. R. George, S. Turner, C. Hawkesworth, et al., "Melting Processes and Fluid and Sediment Transport Rates along the Alaska-Aleutian Arc from an Integrated U-Th-Ra-Be Isotope Study," J. Geophys. Res. **108** (B5) (2003). doi:10.1029/2002JB001916.
18. J. B. Gill, "Orogenic Andesites and Plate Tectonics," (Springer, New York, 1981).
19. G. S. Gorshkov, *Volcanism of the Kurile Island Arc* (Nauka, Moscow, 1967) [in Russian].
20. Y. Goto, M. Nakagawa, and K. Wada, "Tectonic Setting of the Miocene Volcanism in Northern Hokkaido, Japan: Speculation from their K-Ar Ages and Major Element Chemistry," J. Mineral. Petrol. Econ. Geol. **90**, 109-123 (1995).
21. S. Iizumi, K. Maehara, P. A. Morris, and Y. Sawada, "Sr Isotope Data of Some GSJ Rock Reference Samples," Mem. Facult. Sci. Shimane Univ. **28**, 83-86 (1994).
22. S. Iizumi, P. A. Morris, and Y. Sawada, Nd Isotope Data for GSJ Reference Samples JB-1a, JB-3 and JG-1a and the La Jolla Standard," Mem. Facult. Sci. Shimane Univ. **28**, 83-86 (1995).
23. T. Ishikawa and F. Tera, "Source, Composition and Distribution of the Fluid in the Kuril Mantle Wedge: Constrain from Across-Arc Variations of B/Nb and B Isotopes," Earth Planet. Sci. Lett. **152**, 113-122 (1997).
24. O. Ishizuka, R. N. Taylor, A. Milton, and R. W. Nesbitt, "Fluid-Mantle Interaction in an Intra-Oceanic Arc: Constraints from High-Precision Pb Isotopes," Earth Planet. Sci. Lett. **211**, 221-226 (2003).
25. M. C. Jhonson and T. Plank, "Dehydration and Melting Experiments Constrain the Fate of Subducted Sediments," Geochem. Geophys. Geosyst. **13**, 1999. doi:10.1029/999GC000014.
26. P. B. Kelemen, N. Shimizu, and T. Dunn, "Relative Depletion on Niobium in Some Arc Magmas and the Continental Crust: Partitioning of K, Nb, and Ce during Melt/Rock Reaction in the Upper Mantle," Earth Planet. Sci. Lett. **120**, 111-134 (1993).
27. A. B. Kersting, R. J. Arculus, and D. A. Gust, "Lithospheric Contributions to Arc Magmatism: Isotope Variations along Strike in Volcanoes of Honshu, Japan," Science **272**, 1464 -1467 (1996).
28. J.-I. Kimura, M. Kawahara, and S. Iizumi, "Lead Isotope Analysis Using TIMS Following Single Column-Single Bead Pb Separation," Geosci. Rept. Shimane Univ. **22**, 49-53 (2003).
29. J.-I. Kimura and T. Yoshida, "Contributions of Slab Fluid, Mantle Wedge and Crust to the Origin of Quaternary Lavas in the NE Japan Arc," J. Petrol. **47**, 2185-232 (2006).
30. C. H. Langmuir, E. M. Klein, and T. Plank, "Petrological Systematic of Mid-Ocean Ridge Basalts: Constrains on Melt Generation Beneath Ocean Ridges," in *Mantle Flow and Melt Generation at Mid-Ocean Ridges*, Geophys. Monogr. Am. Geophys. Union **71**, 183-280 (1992).
31. V. C. Manea and M. Manea, "Thermal Models beneath Kamchatka and the Pacific Plate Rejuvenation from a Mantle Plume Impact," in *Volcanism and Subduction. The Kamchatka region*, Geophys. Monogr. Am. Geophys. Union **172**, 77-91 (2009).
32. V. C. Manea, M. Manea, V. Kostoglodov, and G. Sewell, "Thermal Models, Magma Transport and Velocity Anomaly Estimation beneath Southern Kamchatka (Chapter 31)," in *Plates, Plumes and Paradigms*, Ed. by G. R. Foulger, D. L. Anderson, J. H. Natland, and D. C. Presnall, Geol. Soc. Am. Spec. Pap. **388**, 388-431 (2005).
33. Yu. A. Martynov, S. I. Dril', A. A. Chashchin, et al., "Geochemistry of Basalts from Kunashir and Iturup Islands: A Role for Nonsubduction Factors in the Genesis of Kuril Island Arc Magmas," Geokhimiya, No. 4, 369-383 (2005) [Geochem. Int. **43**, 328-342 (2005)].
34. A. Yu. Martynov, J.-I. Kimura, Yu. A. Martynov, and A. V. Rybun, "Geochemistry of Late Cenozoic Lavas on Kunashir Island, Kurile Arc," Island Arc **19**, 86-104 (2010).
35. M. T. McCulloch and J. A. Gamble, "Geochemical and Geodynamical Constraints on Subduction Zone Magmatism," Earth Planet. Sci. Lett. **102**, 358-374 (1991).
36. J. D. Morris and J. G. Ryan, "Subduction Zone Processes and Implication for Changing Composition of

the Upper and Lower Mantle," in *Treasure on Geochemistry*, Ed. by R. W. Carlson (Elsevier, Amsterdam, 2003), Vol. 2, pp. 451-470.

37. S. Okamura, R. J. Arculus, and Y. A. Martynov, "Multiple Magma Sources Involved in Marginal-Sea Formation: Pb, Sr, and Nd Isotopic Evidences from the Japan Sea Region," Geology **26**, 619-622 (1998).

38. S. Okamura, R. J. Arcurus, and Y. A. Martynov, "Cenozoic Magmatism of the North-Eastern Eurasian Margin: The Role of Lithosphere Versus Asthenosphere," J. Petrol. **46**, 221-253 (2005).

39. J. A. Pearce, P. E. Baker, P. K. Harvey, and I. W. Luff, "Geochemical Evidence for Subduction Fluxes, Mantle Melting and Fractional Crystallization beneath the South Sandwich Island Arc," J. Petrol. **32** (4), 1073-1109 (1995).

40. J. A. Pearce, P. D. Kempton, G. M. Nowell, and S. R. Noble, "Hf-Nd Element and Isotope Perspective on the Nature and Provenance of Mantle and Subduction Components in Western Pacific Arc-Basin Systems," J. Perol. **40**, 1579-1611 (1999).

41. J. A. Pearce and I. J. Parkinson, "Trace Element Models for Mantle Melting: Application to Volcanic Arc Petrogenesis," in *Magmatic Processes and Plate Tectonics*, Ed. by H. M. Prichard, T. Alabaster, N. B. W. Harris, and C. R. Neary, Geol. Spec. Publ. **76**, 373-403 (1993).

42. J. A. Pearce, R. J. Stern, S. H. Bloomer, and P. Fryer, "Geochemical Mapping of the Mariana Arc-Basin System: Implication for Nature and Distributions of Subducted Components," Geochem. Geophys. Geosyst. **6**, (2005). doi:10.1029/2004GC000895.

43. B. N. Piskunov, *Geological-Petrographic Peculiarity of Island-Arc Volcanism* (Nauka, Moscow, 1987) [in Russian].

44. T. Plank, "Constrains from Thorium/Lanthanum on Sediment Recycling at Subduction Zones and the Evolution of the Continents," J. Petrol. **46**, 921-944 (2005).

45. T. Plank and K. Kelley, "Contrasting Sediment Input and Output at the Izu and Mariana Subduction Factories," Eos, Trans. Am. Geophys. Union, Fall Meet., 82 (2001).

46. T. Plank and C. H. Langmuir, "The Chemical Composition of Subducting Sediment and Its Consequences for the Crust and Mantle," Chem. Geol. **145**, 325-394 (1998).

47. S. Poli and M. W. Schmidt, "Petrology of Subducted Slabs," Ann. Rev. Earth Planet. Sci. Lett. **30**, 207-235 (2002).

48. E. I. Popolitov and O. N. Volynets, "Geochemistry of Quaternary Volcanic Rocks from the Kuril-Kamchatka Island Arc," J. Vocanol. Geotherm. Res. **12**, 299-311 (1982).

49. J. G. Ryan, J. Morris, F. Tera, et al., "Cross-Arc Geochemical Variations in the Kurile Arc as a Function of Slab Depth," Science **270**, 625-627 (1995).

50. K. Shuto, Y. Hirahara, H. Ishimoto, et al., "Sr and Nd Isotopic Compositions of the Magma Source beneath North Hokkaido, Japan: Comparison with the Back-Arc Side in the NE Japan Arc," J. Volcanol. Geotherm. Res. **134**, 57-75 (2004).

51. E. V. Smirnova, I. N. Fedorova, G. P. Sandimirova, et al., "Peculiarities in the Behavior of Rare-Earth Elements in Their Determination in Black Shales by Inductively Coupled Plasma Mass Spectrometry," Zh. Analit. Khimii **58** (6), 595- 603 (2003) [J. Analit. Chem. **58** (6), 533-541 (2003)].

52. E. M. Syracuse and G. A. Albers, "Global Compilation of Variations in Slab Depth Beneath Arc Volcanoes and Implications," Geochem. Geophys. Geosyst. **23** (2006). doi:10.1029/2005GC001045.

53. I. A. Tararin, E. P. Lelikov, and T. Itaya, "Pleistocene Submarine Volcanism in the Eastern Kuril Basin, Sea of Okhotsk," Dokl. Earth. Sci. **371** (3), 366-370 (2000) [Dokl. Earth Sci. **371A**, 494-498 (2000)].

54. M. Tiepolo, P. Bottazzi, S. F. Foley, et al., "Fractionation of Nb and Ta from Zr and Hf at Mantle Depths: The Role of Titanian Pargasite and Kaersutite," J. Petrol. **42**, 221-232 (2000).

55. S. Turner, C. Hawkesworth, N. Rogers, et al., "^{238}U-^{230}Th Disequilibria, Magma Petrogenesis, and Flux Rates beneath the Depleted Tonga-Kermadec Island," Geochim. Cosmochim. Acta **61**, 4855-4884 (1997).

56. *Underwater Volcanism and Zoning of the Kurile Island Arc* (Nauka, Moscow, 1992) [in Russian].

57. J. D. Woodhead and R. W. Johnoson, "Isotopic and Trace Element Profiles across the New Britain Island Arc, Papua New Guinea," Contrib. Mineral. Petrol. **113**, 479-491 (1993).

58. D. Z. Zhuravlev, A. A. Tsvetkov, A. Z. Zhuravlev, et al., "Lateral Variations of Neodymium and Strontium Isotope Ratios in the Quaternary Lavas of the Kurile Island Arc and Their Petrogenetic Significance," Geokhimiya, No. 12, 1723-1736 (1985).

59. T. K. Zlobin, V. N. Piskunov, and T. I. Frolova, "New Data on the Earth's Crust Structure in the Central Part of the Kurile Island Arc," Dokl. Akad. Nauk SSSR **293** (2), 185-187 (1987).